5-18-2023

Willow Abundance and Condition Mapping in Rocky Mountain National Park

Eric M. Nielsen
Portland State University, emn2@pdx.edu

Willow Abundance and Condition Mapping in Rocky Mountain National Park

Eric M. Nielsen
Institute for Natural Resources, Portland State University
Portland, Oregon

May 2023

On this page: A subalpine willow stand dominated by *Salix planifolia* in the Cache la Poudre River valley. Image credit NPS

On the cover: Patchy montane willows in a wet *Calamagrostis canadensis* meadow in Wild Basin, near North St. Vrain Creek. Image credit NPS

Please cite this publication as: Nielsen, E.M. 2023. Willow abundance and condition mapping in Rocky Mountain National Park. Report to the National Park Service, Rocky Mountain National Park.

Contents

Figures

Page

Tables

Appendices

Abstract

Riparian and wetland willow species have undergone serious declines in Rocky Mountain National Park as a consequence of a variety of environmental changes and, most recently, damage resulting from moose overpopulation. To address concerns about the long-term status of willows in the park, we developed remote sensing-based raster maps of riparian and wetland willow species presence, canopy cover percentage, canopy height, and leaf area index. All outputs were produced at 3-meter resolution, and represent willows as they existed in 2021. The mapping was performed via random forests classification and regression models trained on several hundred vegetation plots from a variety of sampling efforts, and making use of predictive layers derived from aerial and satellite imagery, topographic and climatic data. The maps allowed comparison of willow abundance across spatial subsets of the park, including an assessment of areas within ungulate exclosures. Riparian and wetland willow species were mapped as present on 5.45% of the park's total area. Across these areas, most of which likely represent vegetation types where willow is not dominant but only a component, the mean mapped willow leaf area index was 0.694. Accuracy assessment relied on cross-validated model error estimates. The habitat and imagery-based presence classification models with which the willow presence map was created had error rates of 12% and 19% respectively. The regression models for prediction of canopy cover, canopy height, and leaf area index explained 50%, 56%, and 52% of the variance in the dependent variables. The maps will be used to support assessments of willow habitat in the park and (through allometric conversion of leaf area index to leaf biomass production estimates) the determination of summer seasonal moose carrying capacity.

Acknowledgments

Thanks to our many National Park Service cooperators, all of whom were extremely helpful and highly motivated. Hanem Abouelezz, landscape ecologist with Rocky Mountain National Park, initiated and directed this project until her departure from that position in April 2022, and fortunately remained engaged with the work all the way to its completion. She and William Deacy, biologist, provided valuable review and inputs to this manuscript. Chris Clatterbuck managed the project after Hanem's departure and kept things running smoothly.

Allison Konkowski led the field efforts during the 2021 data collection process. Her team of Alliyah Gifford, Ken Yamazaki and Nick Bartush did great work in adapting experimental field protocols to meet unforeseen challenges, and also provided valuable plot quality control assistance. Shawn Wignall and Noah Amme helped with GIS and data management issues. Scott Esser (NPS), David Cooper and Tom Hobbs (Colorado State University) all shared valuable background on natural resource issues and moose–willow interactions in the park. Ray Brunner, vegetation ecologist at the Institute for Natural Resources at Portland State University, took a lead role in developing the field protocol used to collect the 2021 training data.

We made use of plots collected as part of several other projects and programs for this work. Species cover data and vegetation association calls collected in 2002 and 2004 by the Colorado Natural Heritage Program and NatureServe for the Rocky Mountain National Park vegetation classification

and mapping project (Salas et al. 2005) was essential for training the habitat model and for providing willow absence locations across the entire park landscape. Taryn Contento was kind enough to share the willow plot field data she collected in the Kawuneeche Valley for her masters thesis (Contento 2021). Billy Schweiger (ecologist for the NPS Rocky Mountain Network) provided wetland data collected by the network I&M program (see Schweiger et al. 2015) and patiently answered questions regarding its use.

The National Park Service funded this work via the Rocky Mountain Cooperative Ecosystem Study Unit, Cooperative Agreement P21AC10799.

Acronyms

3DEP	3D Elevation Program (USGS digital elevation model purveyor)
AA	accuracy assessment
EVMP	Elk and Vegetation Management Plan
HE	high-elevation willow species group
KV	Kawuneeche Valley
LAI	leaf area index
LE	low-elevation willow species group
LPI	leaf point intercept (transect-based protocol used at some 2021 plots)
NAIP	National Agriculture Imagery Program (USDA)
NVC	National Vegetation Classification
RF	random forests (machine-learning method, Breiman 2001)
RMSE	root-mean-square error
ROMO	Rocky Mountain National Park
SLA	specific leaf area
VCMP	Vegetation Classification and Mapping Project (Salas et al. 2005)

1. Introduction

1.1. Project area

Rocky Mountain National Park (ROMO) occupies 1080 km^2 (107,990 ha; 266,849 acres) in the Rocky Mountains Front Range, about 90 km northwest of Denver, Colorado.[1] The North American continental divide splits the park into eastern and western portions. East of the divide, the northern portion of the park contains the headwaters of the north-flowing Cache la Poudre River. The three primary east-flowing drainages are (from north to south) the Fall River, the upper Big Thompson River, and North St. Vrain Creek. The headwaters of the Colorado River lie west of the divide within the park. The upper Colorado flows south through the Kawuneeche Valley (KV), the dominant feature of the western portion of the park. The southwestern park section drains into Grand Lake and joins the Colorado River just downstream. Elevations within the park range from 2325 m near the town of Estes Park to 4346 m at Longs Peak.

Vegetation within the park is strongly stratified by elevation. According to Salas et al. (2005), the montane zone, found at elevations up to about 3000 m, is characterized by ponderosa pine (*Pinus ponderosa*) and mixed conifer Douglas-fir (*Pseudotsuga menziesii*) forests on the east side. Those forest types are also found on the west side, but lodgepole pine (*Pinus contorta*) and aspen (*Populus tremuloides*) stands are more common in this wetter environment. Above the montane zone, subalpine forests and woodlands dominated by Engelmann spruce (*Picea engelmannii*) and subalpine fir (*Abies lasiocarpa*) are predominant up to about 3320 m elevation. Above tree line, the alpine zone spans another 1000 m of vertical relief. Although they are characterized by upland tree-dominated vegetation, the montane and subalpine zones are each also host to a range of shrubland, herbaceous, and wetland vegetation types (Salas et al. 2005).

We defined the mapping project area by buffering the minimum and maximum extents of the park out by one kilometer, splitting the resulting area into 64 rectangular tiles for parallel processing to increase model prediction efficiency, and keeping only those tiles of which some portion lay within one kilometer of the park boundary. The project area (**Figure 1**) occupies 1496 km^2 (149,616 ha; 369,709 acres) of which the park itself comprises 72%.

[1] Land area and elevation data referenced in this report are derived from NPS GIS data and USGS topographic data, respectively.

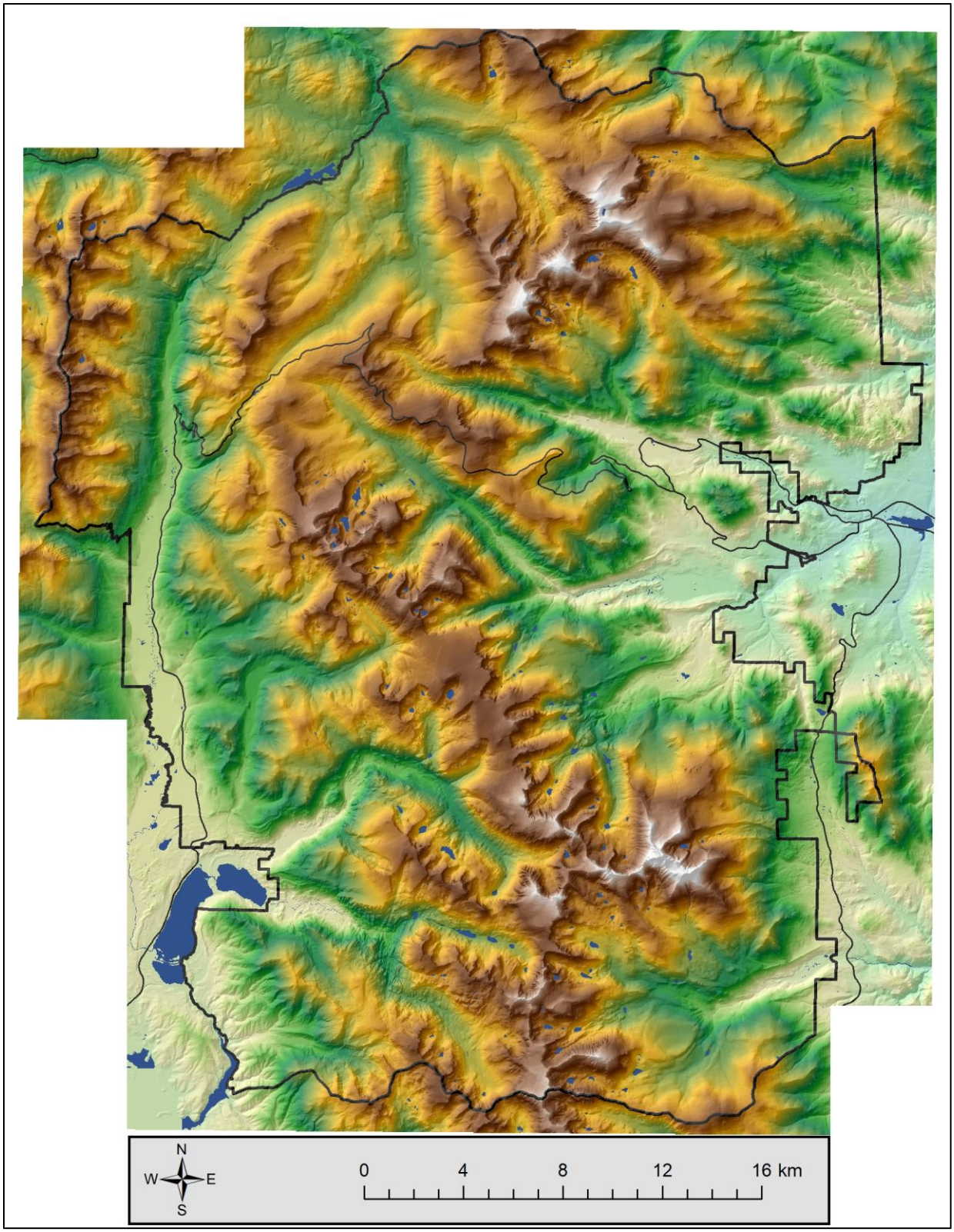

Figure 1. Elevation and water bodies within the mapped area. The park boundary and highways are also shown.

1.2. Willows in Rocky Mountain National Park

Salas et al. (2005) found that willows (*Salix* spp.) constituted the "most diverse and prevalent group of shrublands" within the park. They provided the following review of willow and related wetland and riparian vegetation in the park:

> Wetlands and riparian areas are abundant . . . at all elevations. . . . Near treeline, wet areas are usually home to communities of short willows such as *Salix planifolia* and *Salix brachycarpa*, which often grow mixed with *Betula nana* and dwarfed spruce and fir. Wide riparian valleys in the subalpine zone also contain this mix of shrubs, and often have a diverse understory of forbs and graminoids. Creeks and lakes are abundant in the subalpine: wet meadows and long, thin riparian strips, which often contain tall willows and aspens, can be found near these. In the montane zone . . . riparian vegetation along rivers can be dominated by *Picea pungens* (Colorado blue spruce) or by a mixture of tall willows, aspen and alder. . . . Glacial valley and lakeside meadows are dominated by graminoid species. . . . Willows are often present in strips along streams in these meadows, and occasionally whole valleys can be filled with mixed willow stands.

Salas et al. (2005) identified 27 distinct vegetation associations dominated by willow species. They included these associations within their map units SHRUB–RIPARIAN–CROSS ZONE < 9600 FT (montane zone), SHRUB–RIPARIAN–CROSS ZONE > 9600 FT (subalpine zone), SHRUB UPLAND–ALPINE and HERBACEOUS UPLAND–ALPINE (each of these classes also contain non-willow-dominated vegetation types). The mapped extents of those classes, circa 2001, are shown in **Figure 2**. The KV represents the most extensive montane willow habitat in the park, and the Cache la Poudre headwaters in the north contributes the bulk of the subalpine willow habitat.

Although montane and subalpine willow vegetation types intergrade, they can typically be distinguished based both on species composition and growth forms (D. Cooper, personal communication, 2021). Montane willows typically are found in clumps and primarily reproduce from seed. They live up to 150 years or so, and attain heights up to five meters. Subalpine willows are generally clonal, reproducing primarily via rhizomes. Full-grown individuals are smaller, often only 1.25 m tall. Because of their clonal habit, subalpine willows are more likely to recover rapidly from disturbance than montane willows.

Substantial degradation of riparian willows has been reported in the park since the late 20th century (Kaczynski et al. 2014). Resampling of plots installed in the late 1990s has shown a 30% reduction in willow abundance in the KV (D. Cooper, personal communication, 2021). These changes have been attributed to a variety of causes, such as elk and moose browse, drought, fire, change in water table level, and *Cytospora* fungal infection (see Kaczynski et al. 2014). Most recently, two large wildfires—the Cameron Peak and East Troublesome burns—impacted montane and subalpine willow habitats in the late summer and fall of 2020 (see **Figure 2**).

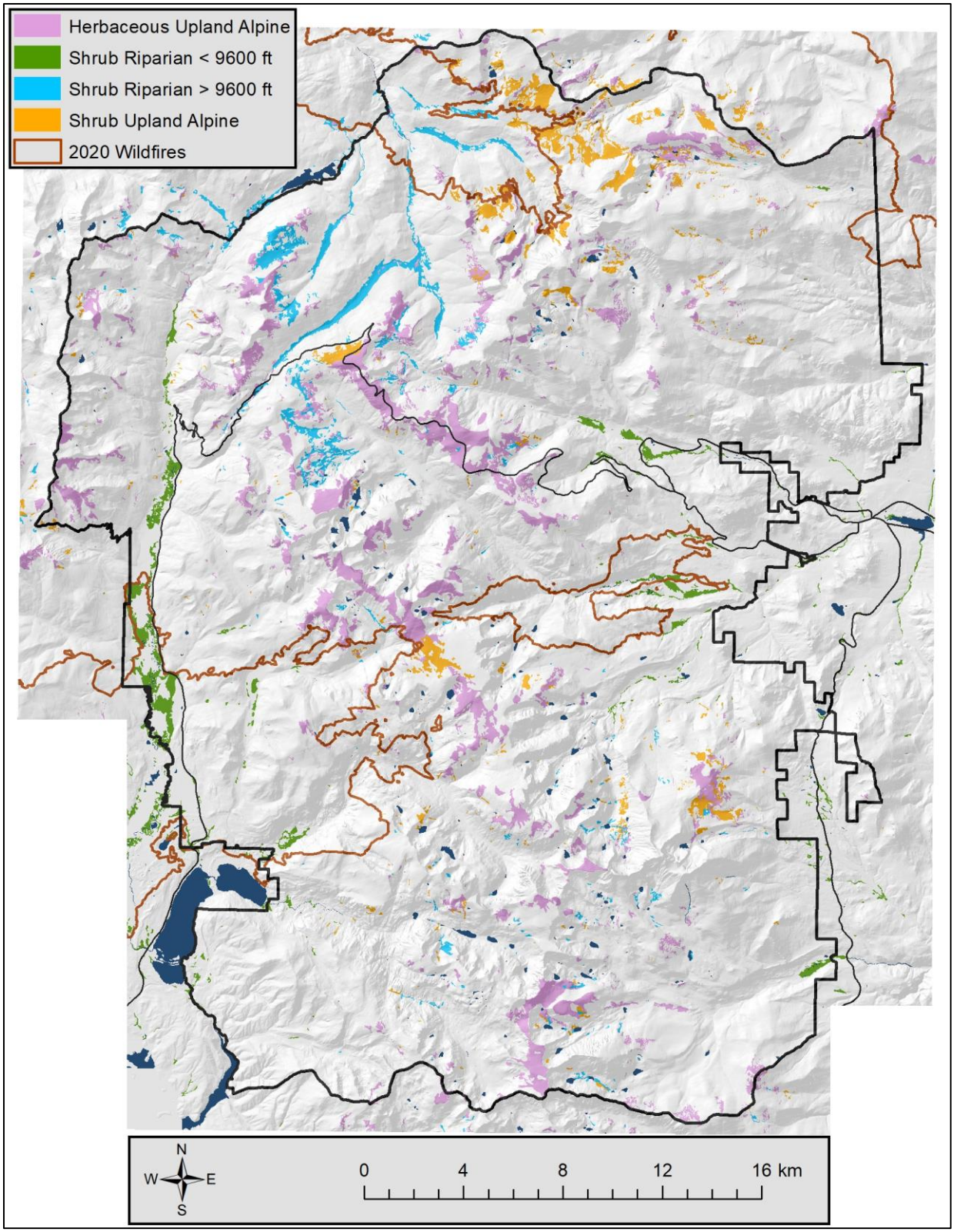

Figure 2. Map units containing willow-dominated associations (Salas et al. 2005), based on imagery collected in 2001. The perimeters of major wildfires in fall 2020 are also shown.

Several willow species which occur in the project area were not addressed in this work. *Salix scouleriana*, a native species primarily associated with upland habitats, and several large non-native tree willow species were dropped from all analyses. In general, when "willow" is referred to in this report, it should be taken to imply only native willows of riparian and wetland habitats.

1.3. Project objective

There is particular concern about the impact of moose on willow stands in the park. Moose tend to develop particular feeding affinities in any geographic region, and at ROMO they rely heavily on willow; montane and subalpine willow species make up over 90% of the summer diet in the KV (Dungan and Wright 2005). There is concern that long-term damage may be done to willow stands in the park as a result of moose overpopulation (T. Hobbs, personal communication, 2021). Better understanding of the willow resource can enhance park management in many other ways, as it is an important restoration focus both in its own right and for the habitat it provides for beaver and other key species (S. Esser, personal communication, 2021). The objective established for this project was therefore to map current willow presence, abundance, and condition within the montane and subalpine zones to support the assessment of willow habitat status and the determination of summer seasonal moose carrying capacity.

Observed patterns of structural spatial heterogeneity from recent field data and the spatial scale at which available ground-truth data had been collected both suggested that a pixel-based map at finer than 5-meter resolution would be needed. We represented willow abundance by mapping willow live canopy cover fraction and willow condition by mapping stand height and mid-summer leaf area index (LAI).[2] All outputs were created at 3-meter pixel resolution. Other possible output metrics (e.g., stem density, above-ground biomass, annual productivity) were considered, but were not feasible given the available ground-truth data. Allometric relationships based on leaf area at the individual or stand scale are a feasible route to producing productivity estimates suitable for use in a carrying capacity analysis.

2. Methods

The requirement for quantitative, self-consistent, and high-resolution estimates of willow abundance and condition suggested use of an automated data-driven remote sensing-based approach. We used machine learning methods to map willow canopy cover, height and leaf area index, and trained models using field observations accumulated from a variety of sampling efforts. The primary phases of the mapping process were a review and incorporation of data from existing willow field plots (**Section 2.1.1**), collection of field data specifically for this project (**Section 2.1.2**), supplementation of these datasets using data from other field efforts (**Section 2.1.3**), generation of additional needed training data via photo-interpretation (**Section 2.1.4**), development of metrics describing willow presence, abundance, and condition from the cumulative field data for use as independent model training data (**Section 2.2**), acquisition of geospatial data and creation of predictive metrics for use as

[2] Leaf area index is a unitless quantity representing the cumulative one-sided leaf area per unit ground area.

model predictor data (**Section 2.3**), mapping of areas disturbed between summer 2020 and summer 2021 (**Section 2.4**), machine learning modeling of plausible willow habitat (**Section 2.5.1**), willow presence (**Section 2.5.2–3**), and willow abundance and condition (**Section 2.5.4**), and post-processing (**Section 2.5.5**).

Because most of the available ground-truth data from the west side of the park was collected in areas later impacted by the 2020 wildfires, it was necessary to do two independent runs of several of the modeling steps (**Sections 2.5.2–4**). The primary run used aerial imagery collected in summer 2019 and Sentinel-2 satellite imagery from summer 2020 before the fires occurred, and made use of all available field data. The secondary run, for use in burned areas, used only Sentinel-2 imagery collected in summer 2021, and made use only of data from plots that were not impacted by fire or other disturbance between summer 2020 and summer 2021. The results from the two runs were fused; results from the primary run were used except in the recently disturbed areas, where they were taken from the more poorly-parameterized secondary run. The fused results can be taken to be generally indicative of post-fire, 2021 conditions. Pre- and post-fire abundance and condition estimates were produced for areas impacted by the wildfires; thus, the impact of the fires on willow communities can be quantified.

2.1. Ground-truth data

We used ground-truth data from a variety of sources for several distinct purposes. The following overview of the data sources includes brief descriptions of the uses made of each dataset. **Table 1** and **Table 2** in **Section 2.1.5** contain a summary of the plot types used for each function and the criteria used to determine which plots would be used from each source. **Section 2.2** and **Section 2.5** have additional information regarding the use of plot data for calibration and modeling tasks, respectively.

2.1.1. Existing willow field data, pre-2021

We began by reviewing the available field data that had been collected in the park for the purpose of monitoring the condition of willow stands. Two main datasets were used: Elk and Vegetation Management Plan (EVMP) willow monitoring plots collected by NPS (Zeigenfuss et al. 2011) and plots collected by Taryn Contento for her masters thesis work (Contento 2021). The pre-2021 willow plot locations are shown in **Figure 3**.

2.1.1.1. EVMP willow monitoring plots

These plots were established at random locations within willow communities, primarily in low-elevation elk winter range on the park's east side (Zeigenfuss et al. 2011). Available data relevant to this work included a willow species list, an assigned **willow type** (a categorical assessment of willow age and height), a set of field photos taken in four cardinal directions, and a set of measurements for each woody shrub with crown overlapping a four-meter square permanent plot (the **macroplot**). The macroplot data included species, percent canopy overlapping the macroplot, live canopy diameter measured in the widest direction and perpendicular to that direction, and the maximum height of the live plant. 121 of these plots had been sampled in 2018. Several additional plots were last visited in 2013, which was too far in the past to be useful here.

The fine spatial grain of the plot data and the fine-scale heterogeneity of willow abundance and condition required that we be sure the plots were well-located with reference to the aerial imagery. NPS analysts verified and if necessary altered the location of macroplot centers by comparing field notes, plot diagrams, and field photos with the 2019 NAIP imagery. Plots were represented as 2.26-meter radius circles for extraction of corresponding predictor data.

2.1.1.2. Contento willow plots

These plots were established in the KV to investigate the influence of herbivory, water table depth, and past agricultural practices on willow productivity. The field data, collected in summer 2020 (Contento 2021), help to close the data gap in montane west-side willow stands. Contento's coarse scale protocol provided data similar to that of the EVMP willow macroplots, with the exception that willow type was not documented. Unfortunately, the spatial accuracy of these plot locations is uncertain. Inspection of several plot locations against aerial imagery indicated there might be considerable spatial offsets. Given the apparent high degree of fine-scale spatial heterogeneity in willow abundance in the KV, spatial uncertainties could result in reliability problems in using these plots as model training data. Several of the southernmost Contento plots were disturbed by fire not long after data collection. Plots were represented as 2.26-meter radius circles for extraction of corresponding predictor data.

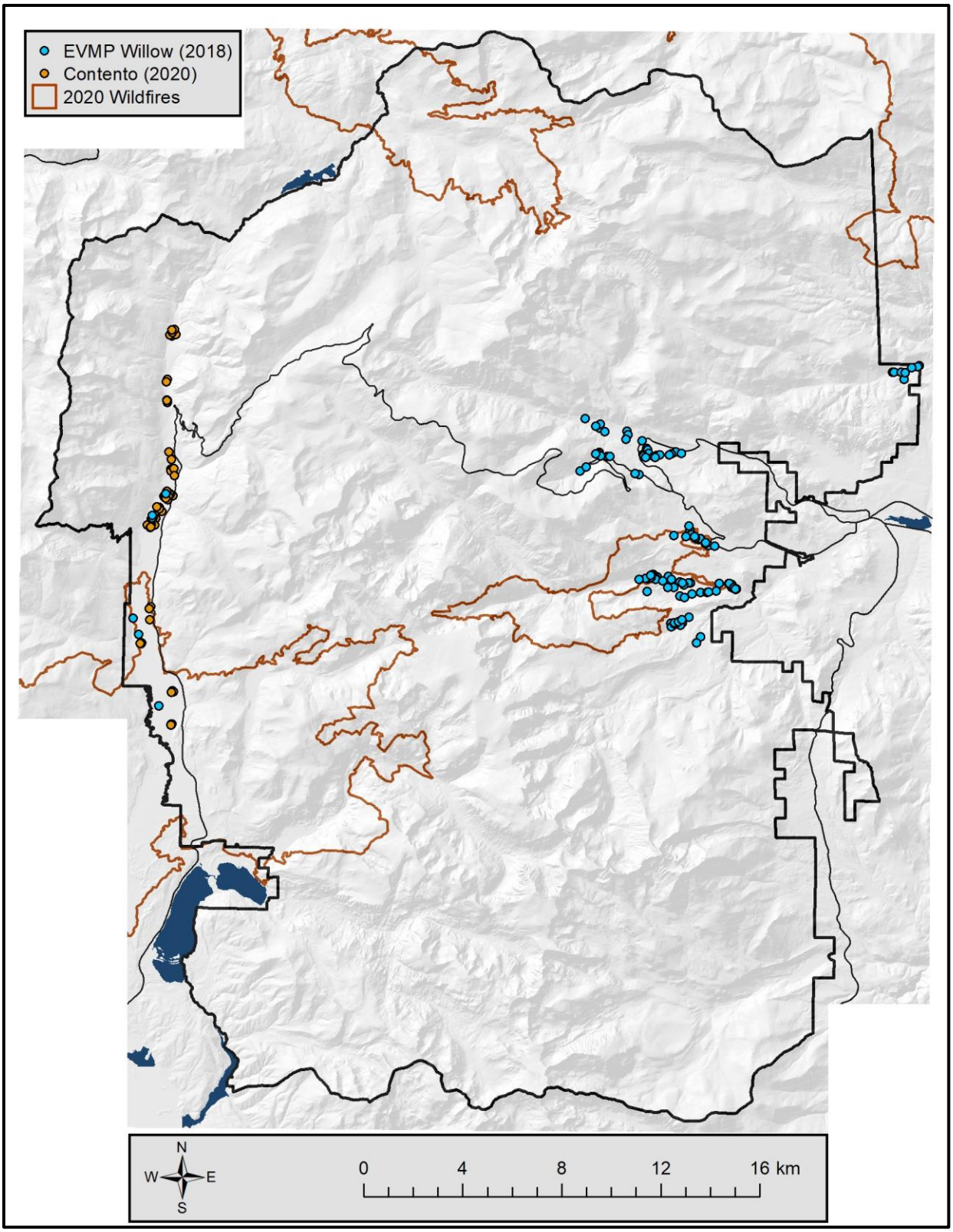

Figure 3. Willow field plots collected prior to 2021.

2.1.2. Targeted field data collection, 2021

Targeted fieldwork for this project was conducted between July 22 and September 22, 2021. The main goals were to obtain plots representing conditions that were poorly sampled in the previously collected willow plots, and to collect additional data that could be used to connect the results of different sampling protocols with each other, allowing their use in a single merged plot dataset. Sampling was targeted in particular geographic areas. Plot locations were not random, but were opportunistically selected in the field in order to most efficiently address data gaps. Priorities included:

- collection of field estimates of willow stand LAI, for use in producing modeled LAI maps which could be converted via allometry to measures of annual productivity;
- collection of plot data representing riparian areas and wet meadows in which willow species are absent (or represent an insignificant proportion of the vegetation), for use in producing modeled willow presence maps;
- collection of plot data in subalpine willow stands, which were not represented in either the EVMP or Contento data;
- collection of plot data in montane west side willow stands, which were poorly represented in the EVMP data and represented with unknown spatial accuracy in the Contento data;
- collection of plot data in Wild Basin, the location of some of the healthiest montane willow stands in the park; and
- resampling EVMP plots located within the 2020 fire perimeters.

In all geographic areas sampled, field crews attempted to establish plots in willow patches and also in similar settings which lacked willow. Accurate mapping of willow presence and abundance depended on having training data available that represented both willow presence and absence, and a range of abundance levels within presence areas. The previously collected plot data contained very few plots in appropriate habitat but lacking substantial willow cover. Therefore, in any particular sampling region, crews were instructed to attempt to collect dissimilar plots representing willow at a range of conditions regarding willow abundance, height, browse impact, and habitat-relevant environmental gradients. Plots were centrally located in homogeneous areas of at ten meters in each dimension, to allow for GPS error and other spatial uncertainties.

2.1.2.1 EVMP macroplot protocol plots

The field protocol (**Appendix A**) generally followed the EVMP willow monitoring methods, with some enhancements. One significant addition to the protocol was the inclusion of visual estimates of percent willow cover over the plot. This allowed the development of a relationship between visual cover estimates and macroplot cover totals, which allowed an increase in consistency of cover estimates across the entire plot dataset.

2.1.2.2. Leaf point intercept protocol plots

Midway through the field season, a collective decision was made that the EVMP macroplot protocol was too time-consuming and would not allow an adequate number of subalpine plots to be collected. In order to speed the field sampling process, we replaced the macroplots with a new leaf point intercept protocol (LPI, see **Appendix B**). The LPI protocol also allowed the estimation of stand LAI, which at that point we had determined was the best field metric for representing annual biomass production (see **Section 2.2**).

The LPI protocol was used in both montane and subalpine willow plots in the latter part of the 2021 field season, and it provided the only source of field-estimated LAI available for use in the project. All LPI plots were collected between August 13 and September 22, 2021; these dates are reasonably compatible with the phenology of peak standing willow crop, which is reached during the latter half of August (T. Hobbs and D. Cooper, personal communication, 2021).

Visual estimates of percent willow cover across plots were also made in LPI plots. These estimates allowed us to extend the link between visual cover estimates and macroplot cover totals, generated from the 2021 macroplots (see **Figure 8**), to LAI estimates from the LPI protocol. This made it possible to develop LAI estimates for macroplots collected before 2021 (see **Table 6**), greatly expanding the pool of LAI training plots.

Thirteen of the LPI plots collected in the KV were revisits of plots established by Contento the previous year. These plots were revisited in order to locate them more precisely—if necessary moving them into more homogeneous adjacent areas—and to provide data for developing a relationship between willow canopy height estimated using the macroplot protocol (used by Contento) vs. that estimated using the LPI protocol.[3] This relationship allowed willow canopy height estimates to be made reasonably consistent across the entire plot dataset, which furthermore allowed macroplot-estimated height to be used in developing LAI estimates for older plots.

NPS analysts verified and adjusted the recorded plot center coordinates of all plots collected in 2021, by comparing field notes, plot diagrams, and field photos with the 2019 NAIP imagery.[4] Plots were represented as 2.26-meter radius circles for extraction of corresponding predictor data. The 2021 targeted field plot locations are shown in **Figure 4**.

[3] Plot coordinates were adjusted by short distances only; field photos allowed us to be confident that the height estimates made in 2020 remained relevant at the new sites.

[4] Although EVMP plots are monumented, many of the coordinates were collected with non-survey-grade GPS units. Accurate co-registration of plot coordinates with the aerial imagery was our primary concern for use of these plots as model training data.

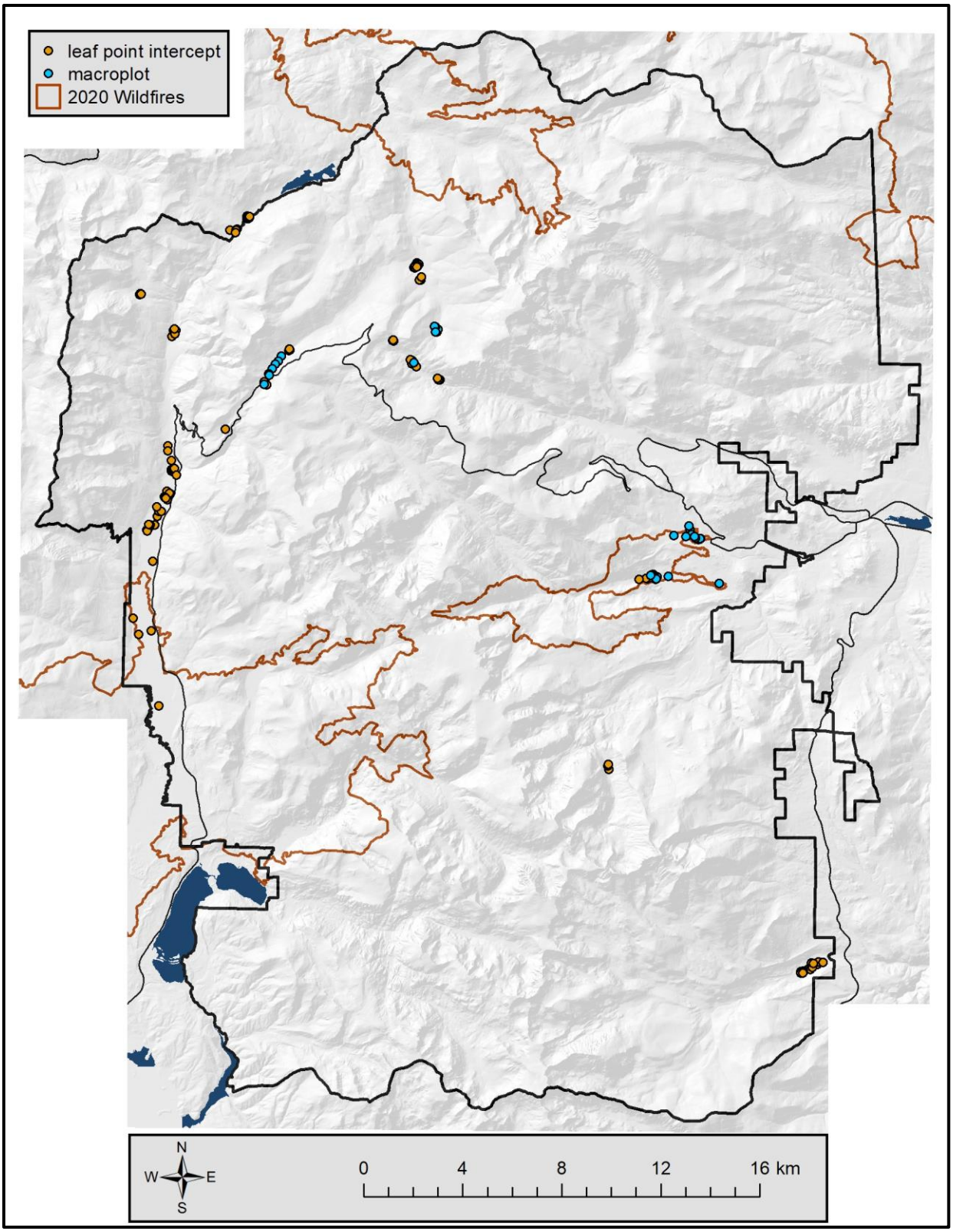

Figure 4. Willow field plots collected in 2021. Early in the season, the EVMP macroplot protocol was used. Later plots used the leaf point intercept protocol discussed in the text.

2.1.3. Data from other field efforts

We imported plots collected for several other projects for use in the map modeling process. These plots were used to improve the delineation of plausible willow habitat within the park, to build models for image-based discrimination of willow presence and absence, and to enhance models of willow canopy cover, height and LAI. In particular, the vegetation association assignments made at the plots collected for the vegetation classification and mapping project (Salas et al. 2005) provided a large set of training samples which lay outside plausible willow habitat. There remained a shortage of plots located in plausible willow habitat but nonetheless lacking willow. Rocky Mountain Network wetland plots (Schweiger et al. 2015), EVMP aspen monitoring plots (Zeigenfuss et al. 2011) and additional classification and mapping project plots were helpful in filling this gap.

2.1.3.1. Vegetation classification and mapping project plots

NPS provided plot data collected during the 2001–2005 vegetation classification and mapping project (VCMP). Salas et al. (2005) describe the collection of relevé plots in 2002 that were used to guide mapping. The plots, most of which were 400 m^2 circles, included a comprehensive species list with visual cover estimates and an assigned vegetation type from the National Vegetation Classification (NVC) as it existed at that time. Additional plots were collected in 2004 for use in accuracy assessment (AA). The AA plots, located in reasonably homogeneous half-hectare sampling areas, included species composition data and an assigned NVC association. Many AA plots were located outside the park boundary, in the buffer area for this project. Fieldwork for both stages was performed by the Colorado Natural Heritage Program and NatureServe. We obtained data for 632 relevé plots and 1223 AA plots. Of these, a total of 1772 plots contained species cover records and a usable association or map unit call.

Using the provided lookup table between associations and map units, we determined the map unit for each plot, and treated plots of the following map units as plausible willow habitat: BLUE SPRUCE, COTTONWOOD, HERBACEOUS WETLAND CROSS ZONE – MARSH, HERBACEOUS WETLAND CROSS ZONE – WETLAND, HERBACEOUS WETLAND SUBALPINE / ALPINE – ALPINE MEADOW, RIPARIAN ASPEN, SHRUB RIPARIAN CROSS ZONE < 9600 FT, SHRUB RIPARIAN CROSS ZONE > 9600 FT, UPPER MONTANE MIXED CONIFER RIPARIAN < 9600 FT, and UPPER MONTANE MIXED CONIFER RIPARIAN > 9600 FT. We also treated plots labeled as the associations *Abies lasiocarpa - Picea engelmannii / Salix (brachycarpa, glauca) Krummholz Shrubland* and *Betula nana - Salix brachycarpa Shrubland*, in the KRUMMHOLZ and SHRUB UPLAND ALPINE map units respectively, as plausible willow habitat.

The VCMP plots used in this project are shown in **Figure 5**. A total of 1279 plots with valid association calls representing implausible willow habitat were used as negative training in the habitat model described in **Section 2.5.1**. Another 335 plots with calls representing plausible willow habitat and which were documented as containing native riparian or wetland willow species (**Section 2.2.1**) were used as positive training in the habitat model. Finally, 170 plots which contained valid species cover data but lacked these species, and which were geographically located in plausible habitat as mapped by the habitat model, were used as negative training in the presence model described in

Section 2.5.2.[5] For extraction of predictor data at plot locations, plots were represented as circles of various radius corresponding to the scale at which the field data had been collected.

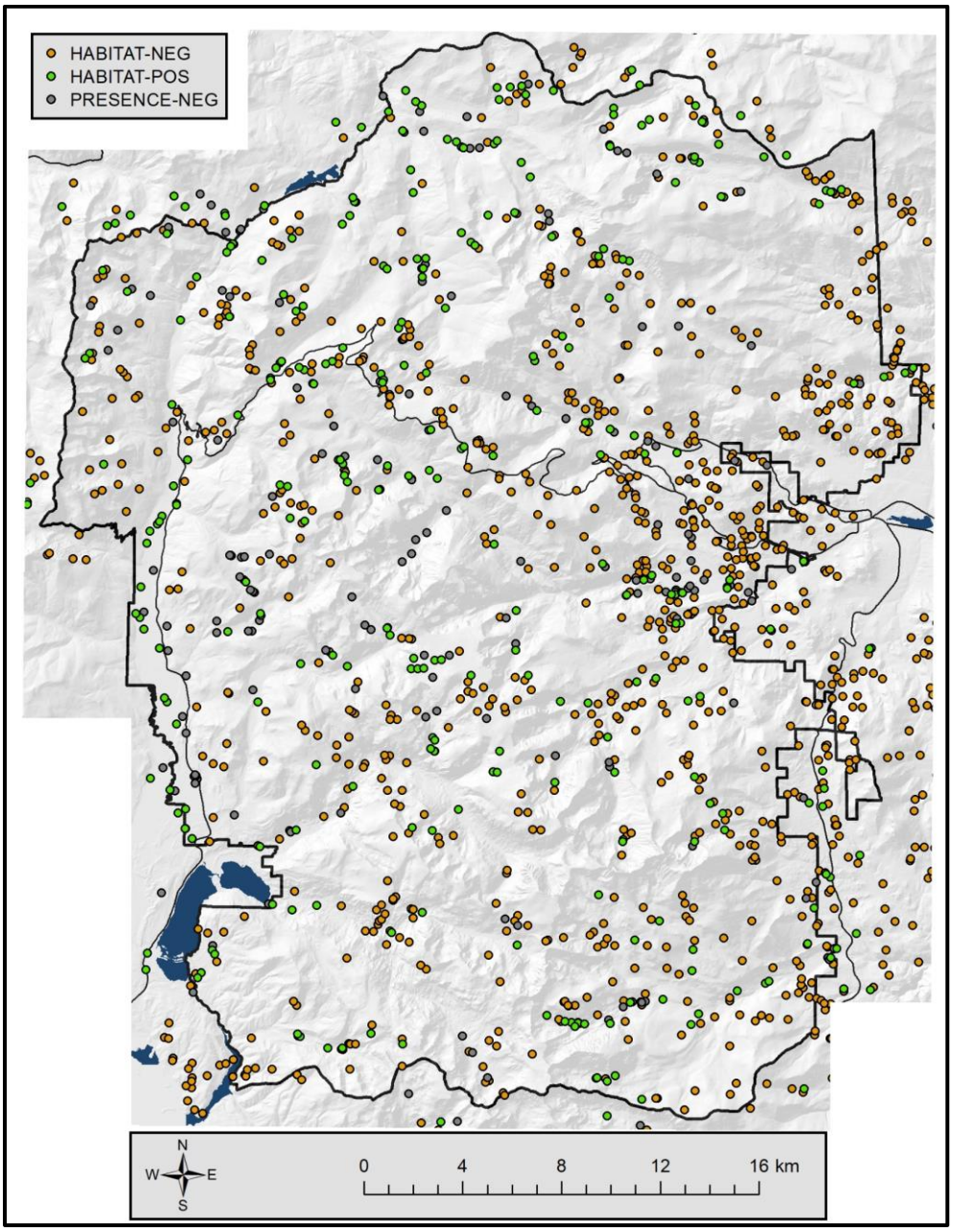

Figure 5. VCMP plots used to model plausible willow habitat and willow presence. POS and NEG plots represent positive and negative training occurrences in the habitat or presence models.

[5] Although these data were collected two decades earlier than the timeframe represented by the maps here, it is thought to be very unlikely that willows have expanded anywhere in the park since this time (H. Abouelezz, personal communication, 2022), so willows are likely still absent in these plots.

2.1.3.2. I&M wetland data

NPS also provided plot data collected for the Rocky Mountain Network long-term wetland monitoring project (Schweiger et al. 2015). We downloaded the data from the NPS IRMA Data Warehouse in July 2021. We dropped older plots, limiting our review to plots collected between 2015 and 2019. The plot locations are shown in **Figure 6**.

We extracted willow cover by species from the dataset's main vegetation table; these were ocular-based estimates of absolute percent cover made over a ten-meter square. We extracted willow height by species from the woody data table. These were measured in the field at the stem scale and can be assumed to be relevant to the species cover estimate in the main vegetation table (W. Schweiger, personal communication, 2022).

Several I&M plots were nearly coincident with EVMP or Contento plots and were dropped, as those were more current. A total of 68 plots were kept; 49 of those contained willows. Wetland plots with documented willow cover were used as positive training data in both the habitat and presence models; plots lacking willow were used as negative training in the presence model but were omitted from the habitat model. For extraction of predictor data at plot locations, these plots were represented as four-meter radius circles, a reasonable compromise considering the scales at which height information was sampled in the field.

2.1.3.3. EVMP aspen monitoring plots

EVMP aspen monitoring plots were collected in both riparian and upland habitats; all of them were revisited in 2018. Their locations are shown in **Figure 6**. Plots were five-meter squares; species cover data were only documented for aspen. We used both types of aspen plots, but for different purposes. The 54 upland aspen plots were used as negative training in the habitat model. Nine riparian aspen plots that contained dense aspen were assumed to not contain significant willow and were used as negative training in the presence model. Plots were represented as 2.82-meter radius circles for extraction of corresponding predictor data.

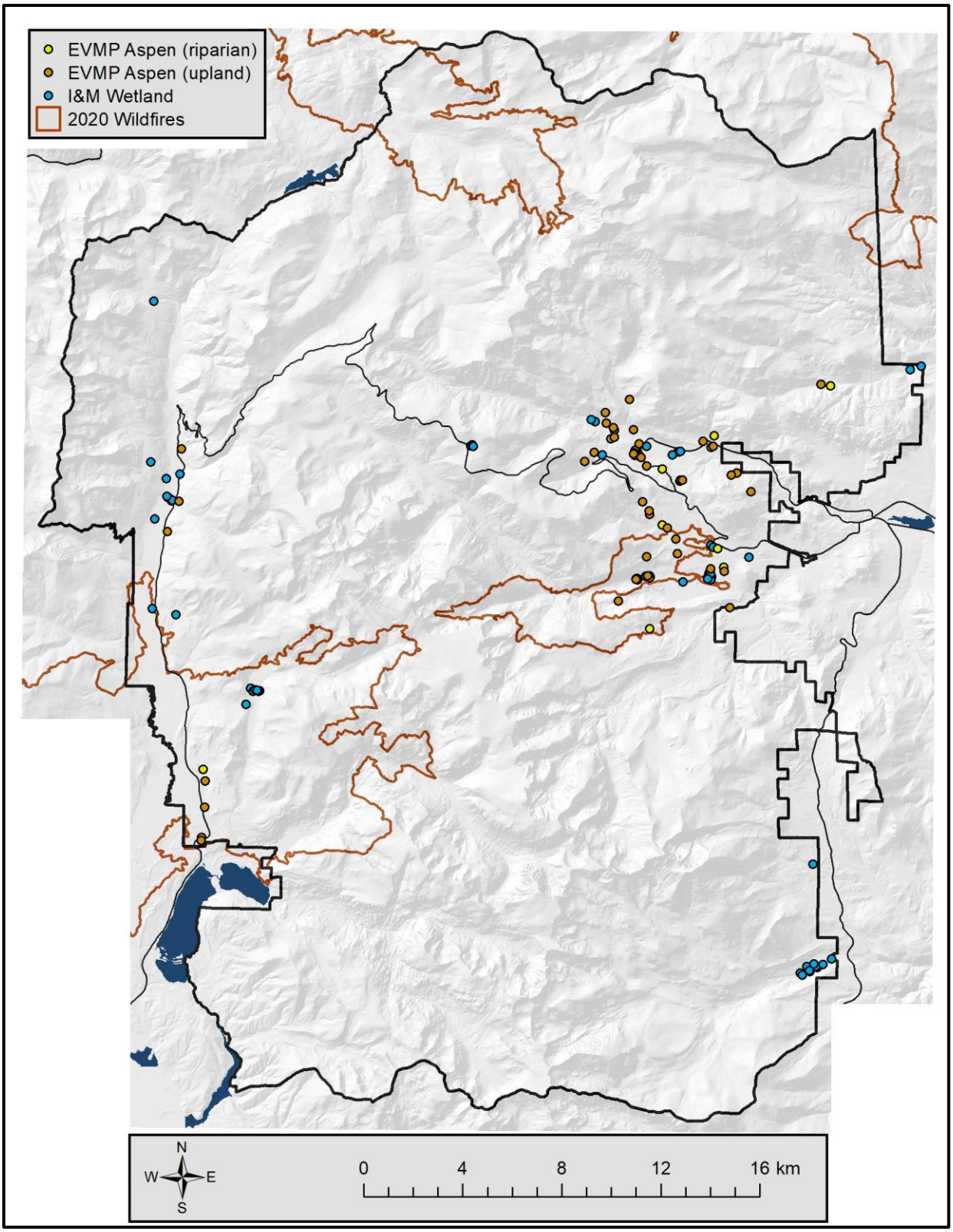

Figure 6. EVMP Aspen and Rocky Mountain Network I&M wetland plots collected from 2015 through 2019.

2.1.4. Remote ground-truth data

2.1.4.1. Photo-interpreted data

Where it was possible to do so confidently, we supplemented the field-collected data by creating additional willow absence plots in land cover types poorly represented in the training data. Several of the alternate land cover types existed only in the buffered area surrounding the park, rather than in the park itself. The plots were photo-interpreted from the 2019 aerial imagery in agricultural fields, developed areas (pavement, golf courses, and residential areas), aspen stands with no indication of willow nearby, open water, unvegetated shorelines, and semi-permanently snow-covered areas. We approached this as an iterative process, assigning additional willow absence locations in areas that appeared to map poorly in previous model runs. Additional plots for the post-fire model runs were photo-interpreted from the 2021 Sentinel imagery to represent burned areas where it was clear no vegetation had survived. The photo-interpreted plot locations are shown in **Figure 7**.

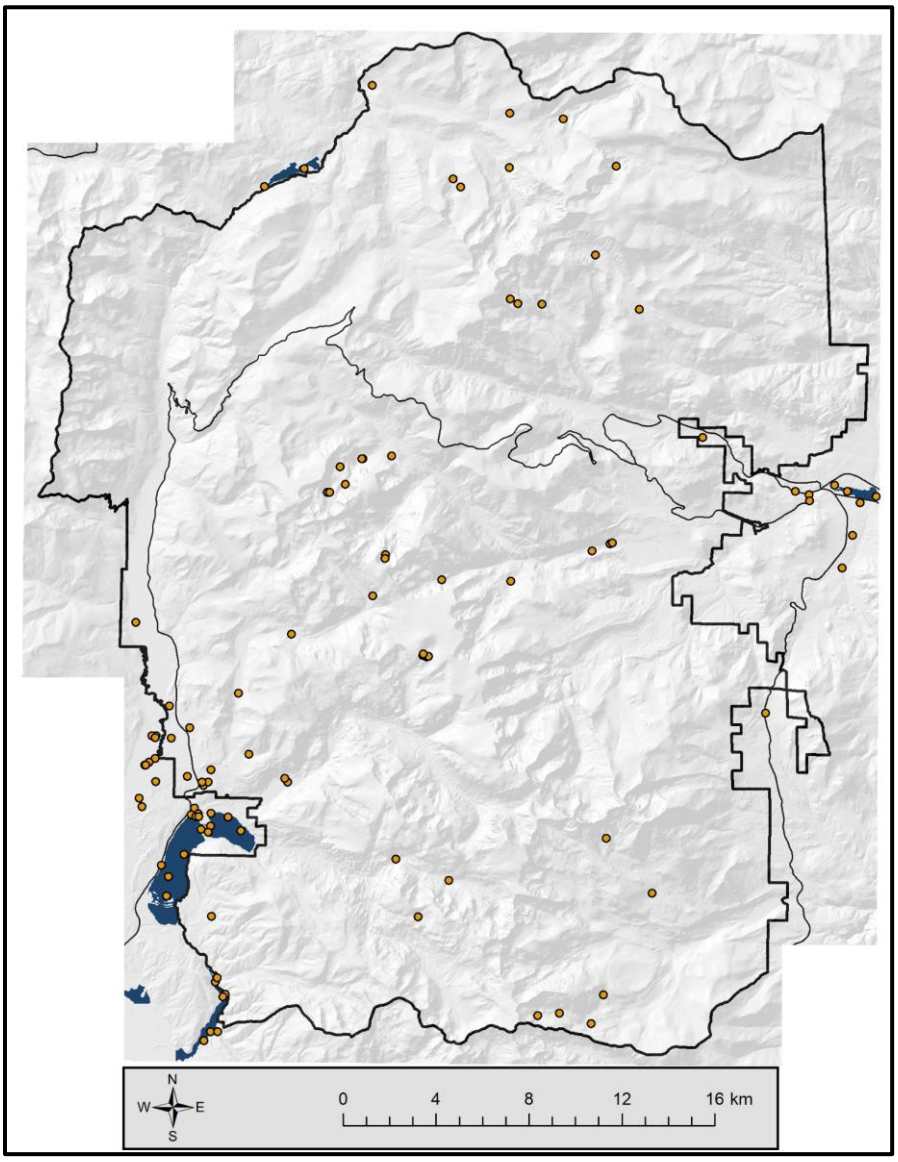

Figure 7. Photo-interpreted plot locations.

2.1.4.2. Lidar data

Lidar data were available for some areas of the park. We had hoped it might be helpful for providing additional training data relevant to willow vegetation canopy. Unfortunately, after evaluating height model outputs from the Moraine Park and Lady Creek collections (visually in Moraine Park, and against Contento's plot data at Lady Creek), we determined the data were likely not informative at the horizontal and vertical scales needed for this application. Data from other collections (e.g., Wild Basin) might have been more useful, had we had more time to devote to the effort.[6]

2.1.5. Plot totals for attributes calibration and model training

The total number of plots used for each of the calibration and modeling tasks, and the inclusion criteria used to select from each sampling effort pool, are described in the following tables. **Table 1** details the plots that were used to develop the calibrations between different estimation methods for cover, height, and LAI, for low- and high-elevation species where applicable. **Table 2** contains the inclusion criteria and plot totals used to develop each of the model phases. Note that the plot counts for the Contento, EVMP willow and targeted datasets vary slightly between models because they contain redundant plots sampled at multiple dates; the most appropriate was chosen for each model.

Table 1. Plots used to calibrate attribute estimates across different plot protocols.

Attribute & function	Type	Source (years)	Inclusion criteria	Plot count
Canopy cover Calibration of EVMP macroplot estimates to ocular estimates **Section 2.2.2**	*low-elevation species*	Targeted (2021)	macroplot protocol, low-elevation willows present	11
	high-elevation species	Targeted (2021)	macroplot protocol, high-elevation willows present	9
Canopy height Calibration of EVMP macroplot estimates to LPI estimates **Section 2.2.3**	*all*	Contento (2020)	willows present, undisturbed in 2020–21	6
		Targeted (2021)	LPI protocol, revisits of Contento plots, willows present	6
Leaf area index Estimation of LAI from ocular cover and LPI height estimates **Section 2.2.4**	*low-elevation species*	Targeted (2021)	LPI protocol, low-elevation willows present, at least one leaf hit recorded	17
	high-elevation species	Targeted (2021)	LPI protocol, low-elevation willows present, at least one leaf hit recorded	47

[6] There are several complications that would arise in using lidar data for training in this project, in any case. Although high point-density lidar can be useful for estimating the structural properties of vegetation canopies as a whole, our mapping targets here are specifically willow species, which could prove difficult or impossible to separate from other woody or even taller herbaceous vegetation in mixed stands. Calibrating lidar-derived cover and height estimates to the estimates available from field-collected plots would present another challenge. Such a calibration could be best accomplished by collecting lidar data over ground-sampled plots reasonably simultaneously with their measurement in the field.

Table 2. Model training data source plots and the dates they represent. The plot counts for the Contento, EVMP willow and targeted datasets vary slightly between models because they contain redundant plots sampled at multiple dates; the most appropriate sample was chosen for each model. Where applicable, post-fire model run totals are shown in parentheses.

Model(s)	Label	Source (reference dates)	Inclusion criteria	Plot count
Plausible habitat **Section 2.5.1**	*positive*	VCMP (2002–04)	willows present, plausible association call	335
		I&M wetland (2015–19)	willows present	47
		EVMP willow (2018)	willows present	89
		Contento (2020)	willows present	64
		Targeted (2021)	willows present	108
	negative	VCMP (2002–04)	implausible association call	1279
		EVMP aspen (2018)	upland type	54
Imagery-based presence pre-fire (post-fire) **Section 2.5.2**	*positive*	I&M wetland (2015–19)	willows present, undisturbed in 2020–21 (post-fire run only)	49 (40)
		EVMP willow (2018)	willows present, undisturbed in 2020–21 (post-fire run only)	96 (89)
		Contento (2020)	willows present, undisturbed in 2020–21 (post-fire run only)	72 (64)
		Targeted (2021)	willows present	99 (106)
	negative	VCMP (2002–04)	willows absent, mapped as plausible habitat (**Section 2.5.1**)	170 (170)
		I&M wetland (2015–19)	willows absent	13 (13)
		EVMP aspen (2018)	riparian type, aspens dense	9 (9)
		EVMP willow (2018)	willows absent	7 (7)
		Photo-interpreted (2019–21)	willows clearly absent	85 (110)
		Contento (2020)	willows absent	28 (28)
		Targeted (2021)	willows absent	33 (29)
Quantitative attributes (cover, height, LAI) pre-fire (post-fire) **Section 2.5.4**	*plot-based estimate of attribute*	I&M wetland (2015–19)	willows present, plot-based estimate of attribute available, undisturbed in 2020–21 (post-fire run only)	48 (39)
		EVMP willow (2018)	willows present, plot-based estimate of attribute available, undisturbed in 2020–21 (post-fire run only)	96 (89)
		Contento (2020)	willows present, plot-based estimate of attribute available, undisturbed in 2020–21 (post-fire run only)	72 (64)
		Targeted (2021)	willows present, plot-based estimate of attribute available	76 (80)
	minimal value of attribute	VCMP (2002–04)	willows absent, mapped as present (**Section 2.5.3**)	77 (44)
		I&M wetland (2015–19)	willows absent, mapped as present	10 (5)
		EVMP aspen (2018)	riparian type, aspens dense, mapped as present	2 (2)
		EVMP willow (2018)	willows absent, mapped as present	5 (0)
		Photo-interpreted (2019–21)	willows clearly absent, mapped as present	24 (13)
		Contento (2020)	willows absent, mapped as present	28 (15)
		Targeted (2021)	willows absent, mapped as present	25 (16)

2.2. Development of training data metrics

NPS and INR agreed to map three local structural attributes of willow: live canopy cover, average live stem height, and peak season LAI. Cover and average height were chosen because they are key structural estimates produced from the EVMP willow monitoring protocol, and are available in some form in all the field plots. LAI was selected because of its strong logical tie to annual biomass production. A particular concern with both cover and height as predictors of annual production is that browse damage and dieback may have weakened connections between these quantities and willow production, and allometric relationships may therefore vary depending on disturbance history. Live canopy cover and live stem height may also become more difficult to estimate accurately in the field under conditions of crown dieback. Furthermore, LAI has the advantage of being a quantity that can be more directly detected in optical (i.e., multispectral) remote sensing data. There is a long history of successful applications mapping LAI using multispectral imagery (e.g., Curran 1983).

Each willow attribute to be modeled across the park requires a substantial set of ground-truth estimates to provide training for model construction. To achieve the needed number of plots, we needed to use plots collected under a number of distinct field protocols. A major goal of the sampling in 2021 was to collect information that could serve to make attribute estimates collected under different protocols compatible with one another. Producing a compatible set of training estimates for each attribute required application of estimated conversion factors, which are detailed for each attribute below.

2.2.1. Assignment of willow species to low- and high-elevation groups

In order to make plot-level estimates of each attribute at a sufficient number of plots to support machine learning modeling, we used empirical methods to create compatible estimates at plots collected using differing field protocols. Recognizing that the differing allometric properties of species might impact the conversions, we lumped species into two broad groups for the purpose of producing compatible attribute estimates. We treated larger willow species, mostly associated with the montane zone, as **low-elevation (LE) willows** and smaller, often clonal, species of the subalpine and alpine zones as **high-elevation (HE) willows**. The LE group was typified by *Salix monticola*, *S. drummondiana* and *S. geyeriana*, while the most prominent HE species were *S. planifolia* and *S. wolfii*.

Before crosswalking all willow records into one of these groups, we first standardized all species records to their current accepted names in the PLANTS Database (USDA NRCS 2023). In keeping with the project objective, we considered only native willows of riparian and wetland habitats. Large non-native trees and willows of upland habitats were dropped from all analysis. We placed species into the elevation groups based on their size, elevation range, and co-occurring species as documented in the various ROMO field datasets. Species entries specifying *Salix* at the genus level were assigned individually based on their size, the plot elevation and co-occurring species. **Table 3** specifies the group to which we assigned each documented species.

Table 3. Lumping of willow species into low-elevation (LE) and high-elevation (HE) groups.

Species	PLANTS code	Group	Justification for dropping
Salix alba	SAAL2	dropped	large non-native tree
Salix babylonica	SABA	dropped	large non-native tree
Salix bebbiana	SABE2	LE	
Salix boothii	SABO2	LE	
Salix brachycarpa	SABR	HE	
Salix drummondiana	SADR	LE	
Salix eriocephala	SAER	LE	
Salix exigua	SAEX	LE	
Salix geyeriana	SAGE2	LE	
Salix glauca	SAGL	HE	
Salix lasiandra	SALA5	LE	
Salix ligulifolia	SALI	LE	
Salix lucida ssp. *caudata*	SALUC	LE	
Salix lutea	SALU2	LE	
Salix melanopsis	SAME2	LE	
Salix monticola	SAMO2	LE	
Salix nivalis	SANI8	HE	
Salix pendulina	SAPE12	dropped	large non-native tree
Salix petiolaris	SAPE5	LE	
Salix petrophila	SAPE18	HE	
Salix planifolia	SAPL2	HE	
Salix reticulata	SARE2	HE	
Salix scouleriana	SASC	dropped	typically found in upland habitats
Salix wolfii	SAWO	HE	

2.2.2. Plot willow cover estimation

Multiple methods of estimating cover were used across the various field plot protocols. We used the ocular live canopy cover estimate that was made on all 2021 plots as our standard, and developed conversions to make estimates made via other protocols compatible.

Cover estimates for LE and HE groups were created at LPI plots by proportionally distributing the total ocular cover estimate into the groups based on the number of leaves intercepted on the transects. For this purpose, the total number of intercepts for each group was increased by one for any member species documented as present in the plot but without any leaf intercepts. We did this to prevent either of the elevation groups from being lost in subsequent analyses by virtue of having been randomly missed in the intercept data.

Macroplot cover estimates for pre-2021 willow plots—calculated as described in Zeigenfuss et al. (2011)—were linked by way of the 2021 macroplot protocol plots. Ocular cover at the 2021 macroplot protocol plots was apportioned into LE and HE willow components based on their proportions in the macroplot cover totals. Separate regression equations were determined for LE and

HE willow species over the plots on which they were present (see **Figure 8**).[7] Those equations were then used to convert pre-2021 macroplot cover estimates to compatible ocular live canopy cover estimates for LE and HE species, which were then summed. Macroplot cover estimates tended to be higher than visual estimates. It is not clear whether this is due to the fact that live canopy does not always fully occupy the ellipse measured in the macroplot protocol, or to a downward bias in the ocular cover estimates. The tendency was more pronounced for HE species.

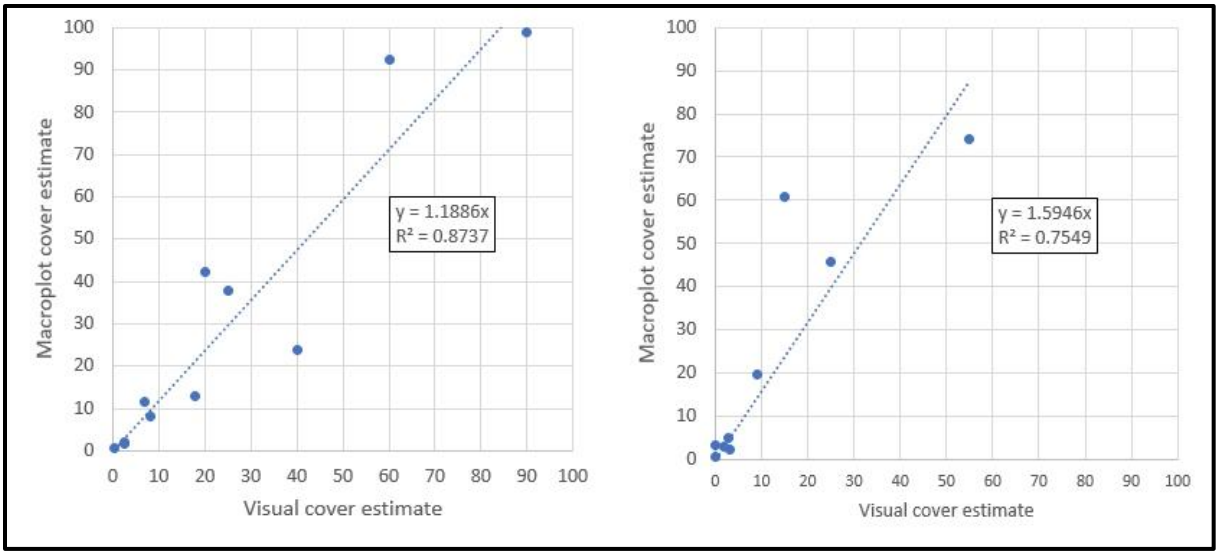

Figure 8. Relationship between species-level visual cover estimate and macroplot cover totals for low-elevation (left) and high-elevation (right) willow species, from 2021 macroplot protocol plots.

Species-level cover estimates at I&M wetland plots were made by averaging continuous-scale ocular estimates over six partially nested subplots (Schweiger et al. 2015). We summed these across LE and HE species groups. We used the dead stems and crown dieback proportion information documented on the woody plant transects[8] to prorate the cumulative ocular cover summed across each elevation group. There were not sufficient co-occurring plots to allow an empirical cover correction to match the 2021 cover estimates, but both methods were based on ocular estimates and the results appeared to be compatible.

[7] **Table 1** summarizes the plots used to develop the regression for each species component.

[8] We produced low- and high-elevation group cumulative dead stem and crown dieback percentage as follows. We first calculated individual plant cumulative dead/dieback percentage as 100 – (*ds* * *cd*) / 100, where *ds* and *cd* are the field-documented dead stem and crown dieback percentages, respectively. We converted the provided individual plant height class to the midpoint of the vertical range for each class, and approximated the fractional cover contribution of each individual *i* on the transect toward the elevation group total as $h_i^2 / \Sigma h_i^2$, where h_i represents the height midpoint of the individual *i* and the sum is performed over all willows in the elevation group documented on the transects. We then multiplied each individual's cumulative dead/dieback percentage by its estimated fractional cover contribution to the group and summed across all individuals in the group.

2.2.3. Plot willow height estimation

Multiple methods of estimating height were used across the various field plot protocols. We used the maximum LPI leaf intercept height recorded for each of the elevation species groups as our standard, and developed conversions to make estimates made via other protocols compatible. The maximum LPI height intercepted on the 16 points is a reasonable proxy for the height of the upper canopy as it represents an estimate of the 94th percentile top-of-canopy height. An overall stand height estimate was produced by combining the LE and HE groups' height estimates proportionally to their representation in their adjusted leaf intercept counts. No height estimates were available for 20 of the 88 LPI plots with willow present, because no leaves were contacted at any of the intercept points. Only four of these plots had ocular cover estimates of five percent or more. Two plots had cover estimates of ten percent. These plots were collected on September 21–22 and the willows appear to lack leaf cover in field photos; at each of these plots, the crew noted that willow leaves were "falling off," "dead" or "dying."

Macroplot height estimates for pre-2021 willow plots and 2021 macroplot protocol plots were calculated by averaging the heights of all willows within the macroplot (Zeigenfuss et al. 2011). These estimates were linked to the LPI height standards by way of plots measured by Taryn Contento in 2020 using the EVMP macroplot protocol and resampled in 2021 using the LPI protocol. The plots selected for inclusion were carefully examined to ensure the resampled plots had been collected on the same willow stands that Contento visited in 2020. The remeasurements allowed us to generate an empirical relationship between the two height estimation methods (**Figure 9**).[9] Macroplot height averages tended to be higher than LPI maximums, as they were derived from the maximum live height of each plant, while point intercepts simply represent a uniform sample of the canopy as a whole.

[9] **Table 1** summarizes the plots used to develop the regression. Sufficient data were not available to generate independent relationships for LE and HE species groups. The remeasured plots were all located in the KV. Additional remeasurements from other parts of the park would have been helpful. Not only was the number of plots limited, but the small number of samples on the point intercept transects resulted in a high sampling error.

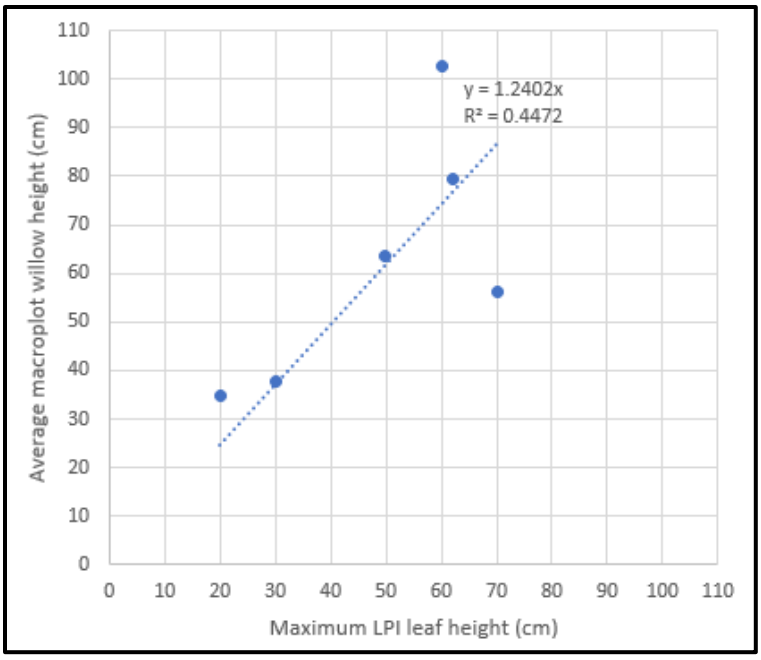

Figure 9. Relationship between height estimated using macroplot averages vs. LPI maximum, from revisited Contento plots.

Height estimates at I&M wetland plots were derived from the woody plant transects, along which individual plants were assigned height classes. We estimated the height of each individual as the midpoint of its height class, and summarized similarly to the macroplot data, by simply averaging all documented individuals. With no source of calibration data, we used the same multiplier (generated from **Figure 9**) we had used to adjust the macroplot height estimates.

2.2.4. Plot leaf area index estimation

Direct LAI measurements were made only at the 2021 LPI protocol plots. To generate LAI estimates for all other plots we used the LPI protocol data to define a predictive formula for LAI based on stand-level willow cover and height. We generated this relationship separately for LE and HE species groups because of their differing physiognomy.

2.2.4.1. Calculation of leaf area index at LPI plots

Stand-level LAI was estimated based on the number of leaves intercepted on the LPI transect. At each point, a local LAI was estimated by multiplying the leaf count by a correction factor based on visually estimated average leaf angle from the horizontal:

$$LAI_{point} = \frac{c_{point}}{\cos(\min\{\alpha, 60\})} ,$$

where c_{point} represents the number of leaves intercepted at the point and α is the average leaf angle from the horizontal, given in degrees. At very high leaf angles, the denominator becomes extremely small; we chose to limit the LAI estimate to realistic quantities by allowing a maximum of 60

degrees for the leaf angle estimate.[10] The stand-level LAI was computed by averaging the 16 point LAI estimates.

2.2.4.2. Estimation of leaf area index at other plots

A total of 50 LPI plots were collected in montane habitat. LE willows were absent at 14 of these plots; another 17 plots had small amounts of LE willow but none recorded on the LPI transects. We eliminated two plots which had inconsistent data or were located in excessively heterogeneous areas. No subalpine habitat plots contained LE willow species. 17 plots remained for developing a predictive relationship for LE willow LAI in terms of cover and height. These plots had cover values ranging from 4% to 95%, height from 20 to 360 cm, and LAI from 0.1 to 9.9 (see **Table 4**).

A total of 61 LPI plots were collected in subalpine habitat. HE willows were absent on 14 plots, and another eight plots had small amounts of HE willow but none recorded on the LPI transects. An additional eight LPI plots in the montane zone contained non-zero LAI estimates for HE willows. 47 total plots were available for developing a predictive relationship for HE willow LAI in terms of cover and height. These plots had cover values ranging from 2% to 75%, height from 10 to 130 cm, and LAI from 0.1 to 3.2 (see **Table 4**).[11]

For comparison to **Table 4**, **Table 5** contains the cover and height characteristics of the current-era plots with low- and high-elevation willow species present. Locations of the plots used to generate the predictive relationship for LAI are shown in **Figure 10** for both elevation species groups.

Table 4. Cover, height and leaf area index characteristics of the plots used to form the predictive relationships for LAI. The low-elevation group had 17 plots; the high-elevation group had 47.

Variable	Group	Minimum	1st quartile	2nd quartile (median)	3rd quartile	Maximum
Cover (%)	LE	4	10	25	45	95
	HE	2	6	22	43	75
Height (cm)	LE	20	40	70	310	360
	HE	10	25	40	60	130
Leaf area index	LE	0.1	0.3	0.5	4.7	9.9
	HE	0.1	0.4	0.9	1.4	3.2

[10] Limiting the leaf angle estimate to a maximum of 60 degrees from the horizontal introduces a downward bias on LAI estimates on the rare occasions angles greater than that limit were documented in the field. In practice, the limit served to counter the extreme reaction of LAI estimates to comparatively small over-estimates of angle under high leaf-angle conditions; affected plots retained very large LAI estimates despite the limitation. The need to estimate leaf angle is a major shortcoming of this sampling method; an alternative field approach is proposed in **Section 3.5**.

[11] **Table 1** summarizes the plots used to develop the regressions for each species component.

Table 5. Cover and height characteristics of the current-era plots with willow species present.

Variable	Group	Minimum	1st quartile	2nd quartile (median)	3rd quartile	Maximum
Cover (%)	LE	< 1	4	14	45	170
	HE	< 1	2	5	18	81
Height (cm)	LE	19	42	75	147	410
	HE	9	25	45	73	305

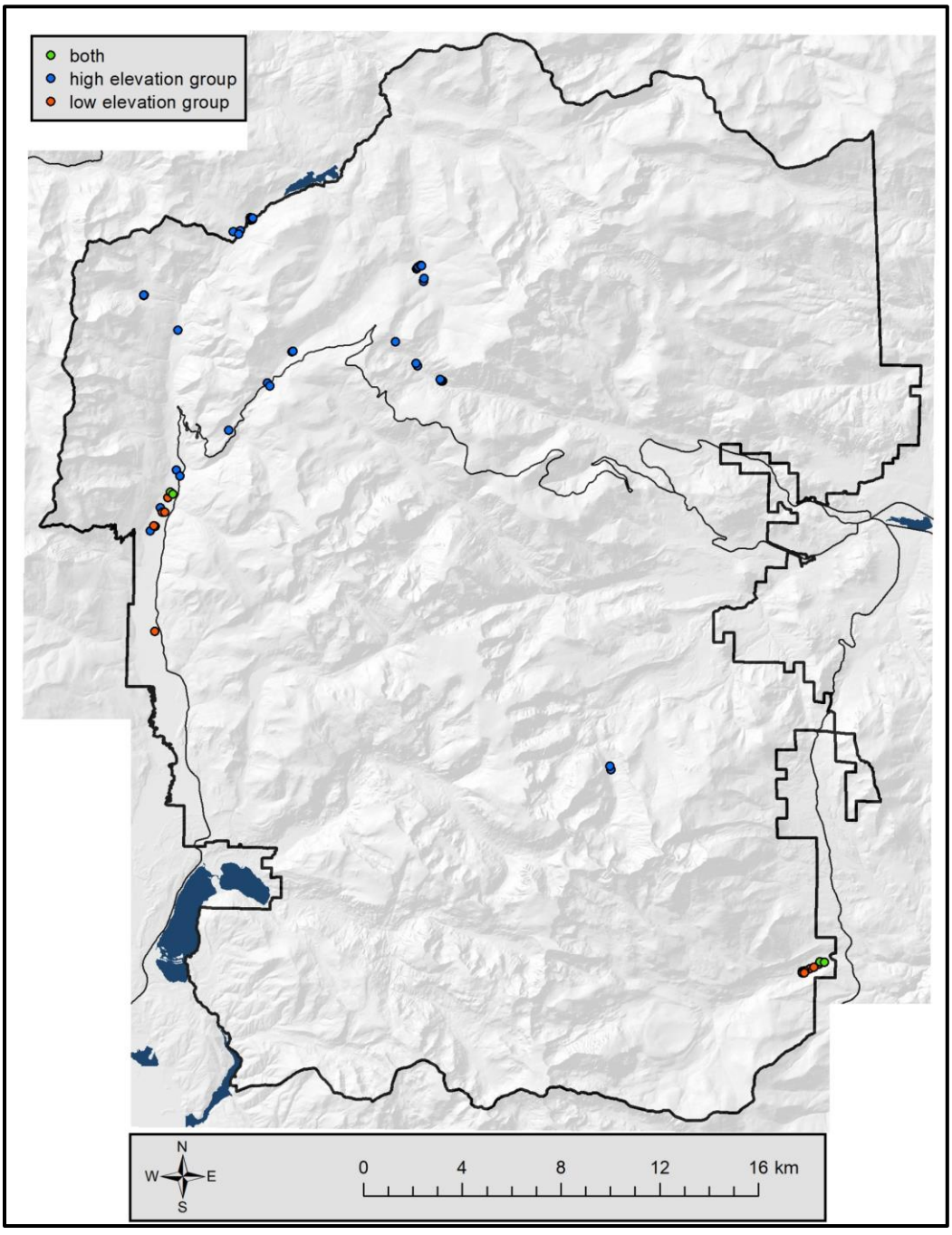

Figure 10. LPI plots used for prediction of leaf area index from cover and height data, for low- and high-elevation species groups. Four plots provided data for both groups.

For each elevation species group, we created linear regression models for LAI on cover and height, and for LAI on cover alone (**Table 6**). Based on the reported statistical significance of the coefficient estimates for the independent variables, we selected model L2 for the LE group and model H1 for the HE group. Therefore, the LAI of LE species at non-LPI plots was calculated based on cover alone, while the calculation of HE species LAI used both cover and height as predictors.

Table 6. Regression results for dependent variable leaf area index on independent variables cover and height. The constant term was set to zero. The models marked with '*' were selected for use in predicting LAI from measured quantities at all plots other than 2021 LPI protocol plots.

Independent variable, parameter		L1: Low-elev group, cover & height	*L2: Low-elev group, cover only	*H1: High-elev group, cover & height	H2: High-elev group, cover only
Cover (%)	coefficient estimate	0.0798	0.0722	0.0216	0.0360
	significance	p < 0.001	p << 0.001	p << 0.001	p << 0.001
	standard error of estimate	0.0172	0.0059	0.0044	0.0023
Height (cm)	coefficient estimate	-0.0019	—	0.0109	—
	significance	p = 0.643	—	p < 0.001	—
	standard error of estimate	0.0041	—	0.0029	—
R-squared		0.9058	0.9044	0.8744	0.8360
Adj R-squared		0.8933	0.8985	0.8689	0.8324
Number of obs		17	17	47	47

2.3. Generation of model predictor data

We assembled a collection of wall-to-wall rasters for use as model predictor data. The predictors fell into four broad categories: (a) metrics derived from high-resolution aerial imagery, collected in summer 2019; (b) metrics derived from medium-resolution satellite imagery, collected in 2019–2021; (c) topographic and hydrologic metrics developed from digital elevation models; and (d) climate normals over the period 1991–2020. Hydrography, soils and surface geology data were considered for use but ultimately rejected. We felt their use would result in mapping artifacts and add little predictive power, since highly correlated information was available already in the other predictors. Lidar data, which might be used to provide information relevant to vegetation canopies and more precise topographic information, are available for some areas of the park, but were not relevant for use in this park-wide application.

An effective spatial resolution was estimated for each predictive metric. This quantity represents the responsiveness of the metric to spatial land cover heterogeneity, and is influenced both by the resolution of the data source and by the dimensions of any convolution kernels used in the metric

calculation process.[12] Effective spatial resolution of metrics were used later in the predictor selection process to simultaneously optimize model error rate and spatial responsiveness. All analysis steps below were performed in **Python 2.7** (Python Software Foundation 2010) or in **R 4.0.2** (R Development Core Team 2020).

2.3.1. Aerial imagery

We used 4-band color-infrared imagery collected in summer 2019 by the National Agricultural Imagery Program (NAIP). The 60-centimeter resolution imagery was obtained as uncompressed quarter quads. We used the imagery to calculate a variety of metrics representing spectral response and spatial patterning. Two main types of metrics were produced. Reflectance metrics are calculated at the scale of a single imaged pixel; these represent both raw band responses and nonlinear multiband combinations. Multiscale nested texture metrics (Nielsen and Noone 2014) are based on local moving window variability in spectral response, computed on image pixels resampled to a variety of different image resolutions. The metrics described in Nielsen et al. (2021) were produced across the project area and summarized at 3-meter resolution.

2.3.2. Satellite imagery

Sentinel-2 satellite reflectance data were obtained for the project area using Google Earth Engine (Google 2021). A medioid compositing method was used to create Sentinel-2 mosaics over monthly intervals, removing clouds, cloud shadows and other corrupt data from the individual images. Composites were created for each month from June through September, and each year from 2019 thru 2021. Images from outside the seasonal window were mostly snow-covered or had very low sun angles. The red, green, blue, near-infrared and two shortwave infrared bands were obtained in this way at their native 10-meter or 20-meter resolution. All data were resampled to 10-meter resolution using a cubic convolution resampling method.

The monthly composites were visually inspected using a variety of band combinations and contrast stretch options. Several of the monthly composites were impacted by clouds, cloud shadows, smoke, snow at higher elevations, and other compositing noise. Upon review, the July 2020 and September 2019 composites were selected as the best images for the pre-fire period, while August 2021 and September 2021 were the best images in the post-fire period. The July 2020 and August 2021 composites were used for change detection over the summer 2020–summer 2021 time period. A wide variety of spectral indices were created from the reflectance data in the four selected composites; the metrics are reviewed in Nielsen et al. (2021).

2.3.3. Topographic data

We downloaded 10-meter resolution elevation data for the project area from the 3D Elevation Program (3DEP; USGS 2021). For processing efficiency, the elevation data were converted to integer format using a vertical unit of 0.25 feet. A wide variety of metrics describing aspects of local

[12] For example, effective spatial resolution of a metric describing local variability in spectral response is influenced both by the source image resolution and by the window size over which variability is estimated.

topography that often influence vegetation abundance and composition were created from the elevation data; the metrics are reviewed in Nielsen et al. (2021). We also derived hydrological flow paths and a resulting channel network from the elevation data, using USGS 24k topographic quads to calibrate channel initiation flow thresholds. We used the resulting network and hydrological flow information to compute a range of additional metrics describing the local influence of hydrology. These metrics and their methods of creation are also reviewed in Nielsen et al. (2021). We used SAGA-GIS (Conrad et al. 2015) for some of the hydrological analysis.

2.3.4. Climate data

We downloaded a range of monthly 30-year (1991–2021) climate normals at approximately 800-meter resolution from the PRISM Climate Group (2021), including precipitation, minimum and maximum temperature, mean dew point temperature, and minimum and maximum vapor pressure deficit. All normals were obtained for the months of January, April, July and October; for each metric, we averaged these four months to approximate an annual average.

2.3.5. Resampling and data reduction

All metrics were resampled to a fixed 3-meter resolution grid over their coincident extent. The resampling method used depended on the data source. We used nearest neighbor resampling to maintain the finest resolution possible for all metrics derived from aerial imagery; the predictor sampling grid was taken from these rasters to prevent any spatial shifting. Satellite imagery was resampled using cubic convolution, which results in less smoothing than bilinear interpolation and maintains crisper boundaries. The non-imagery layers were resampled using bilinear interpolation.

We used the R **caret** package (Kuhn 2008) to reduce multicollinearity within each of the four predictor categories separately. For each pair of predictors with absolute-valued Spearman rank correlation above a certain threshold, the predictor with the largest mean absolute correlation (to all other remaining predictors) is discarded. This has the effect of removing highly correlated predictors, while keeping those which are most unique among the full predictor set. Correlations were calculated across the set of training plots, which varied for each model. The threshold correlations used were $\rho = 0.8$ ($\sim R^2 = 0.64$) for climate predictors, $\rho = 0.7$ ($\sim R^2 = 0.49$) for topographic predictors, $\rho = 0.8$ ($\sim R^2 = 0.64$) for satellite imagery predictors, and $\rho = 0.65$ ($\sim R^2 = 0.42$) for aerial imagery predictors. Different thresholds were used to introduce some balance in the number of selected predictors between the different groups; all were in keeping with the range of recommended values.

2.4. Mapping of recently disturbed areas

The 2020 fires rendered the 2019 aerial imagery obsolete for use in making current willow maps in impacted areas. Because models making use of the aerial imagery were significantly more accurate than those relying solely on Sentinel-2 data, we aimed to minimize the extent of the project area mapped without aerial imagery. To accomplish this, we mapped disturbance at the pixel scale rather than simply using outer burn perimeters to determine which model would be used for a given location. Note that other minor disturbances impacted some portions of the park between summer 2020 and summer 2021; the approach we used also handles those areas appropriately.

We flagged areas impacted by fire or other disturbance in the interval between July 2020 and August 2021 using a change detection method based on Sentinel-2 imagery. We used the ArcGIS Iso-Cluster Unsupervised Classification function to create 50 distinct spectral clusters from a six-band stack consisting of the red (B04), near-infrared (B8A), and mid-infrared (B11) bands from the July 2020 and August 2021 Sentinel-2 images, and manually assigned each of the clusters to change or no-change based on visual inspection of the Sentinel-2 and aerial imagery. Nearly all the changed areas were located within the burn perimeters. Areas modeled as disturbed in the 2020–2021 interval are shown in **Figure 11**.

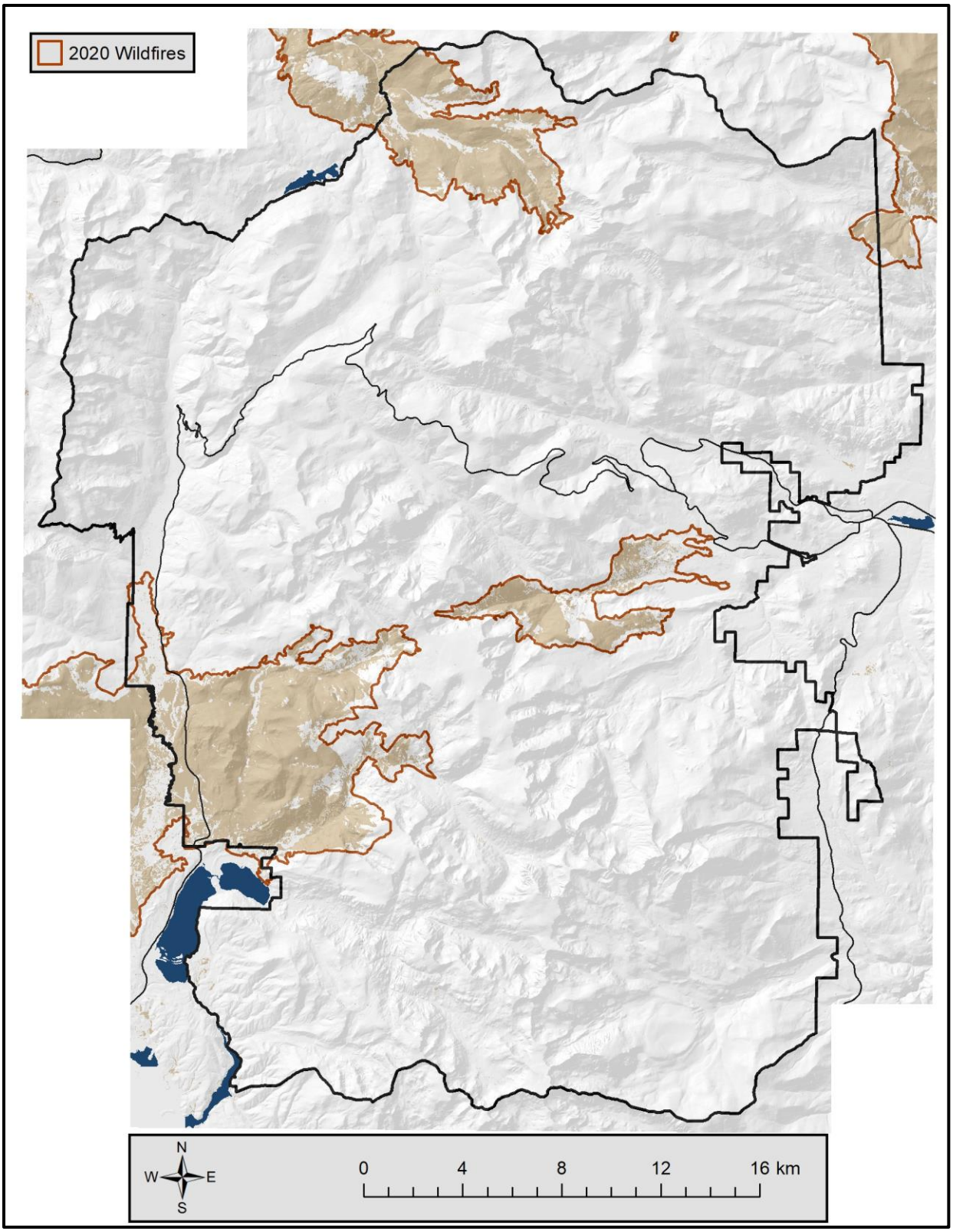

Figure 11. Shaded areas represent disturbance between summer 2020 and summer 2021. Within these areas, final maps were derived from models based on 2021 satellite imagery, rather than on aerial and satellite imagery from 2019–20.

2.5. Willow mapping

The map modeling process was tackled in three phases. First, we mapped the likelihood that any 3-meter pixel comprised plausible willow habitat, where the topographic and climatic setting are likely within the envelope occupied by willow species. Second, we mapped the level of confidence with which willows were detected in aerial and satellite imagery. We combined the results of the habitat and image-based willow detection models into a single joint likelihood of willow occupation at each pixel.[13] Third, for all pixels with willows present, we mapped quantitative estimates of live canopy cover percent, canopy height and LAI. We performed additional runs of the willow detection and quantitative models to represent post-fire conditions; the outputs of these runs were used only in areas that were flagged as disturbed between summer 2020 and summer 2021.

Different sets of plots were used as training data for these distinct tasks. The habitat model relied heavily on the VCMP plots which were collected across a wide variety of habitats in the park. For the imagery-based mapping tasks—the willow presence and attributes models—we identified and excluded from training data any plots that the disturbance mapping identified as changed between their sampling date and the acquisition date of the imagery used in modeling.

For all modeling tasks, we used the R language implementation (Liaw and Wiener 2002) of the random forests (RF) machine learning algorithm (Breiman 2001). The RF classification algorithm was used for habitat and presence modeling, and the cover, height and LAI mapping used RF regression. We used RF because of its tendency to avoid overfitting to training data and its ability to isolate signals in noisy datasets (Cutler et al. 2007). We used a predictor selection algorithm that reduced prediction time and co-optimized model accuracy and effective spatial resolution.[14] We made use of the R **raster** (Hijmans 2018) and **rgdal** (Bivand et al. 2014) packages throughout.

---

[13] Habitat and image-based detection were modeled in two separate steps to permit the formation of well-balanced models trained on two distinct knowledge bases. Because willow is thought to have declined significantly since their collection, EVMP plots could not be used to provide positive willow presence information relevant to current imagery. However, relying only on modern-era plots to provide positive willow presence data to a model aware of environmental setting would have encouraged the mistaken conclusion that willows do not occur outside the environmental envelope over which the EVMP willow and I&M wetland plots were sampled. Breaking the modeling up into two steps allowed the use of EVMP willow occurrence data over the habitat-specific domain where they are relevant.

[14] For the classification models, the out-of-bag error rate for each plot was compiled over each of the forests and converted to an estimate of the probability of plot misclassification by a single forest. This quantity, averaged over all plots, was used to stepwise select for additional predictors in the model, moving successively through tiers of predictors ordered by their effective spatial resolution. For the regression models, predictor selection optimized model accuracy by minimizing the sum of out-of-bag root mean square error and mean absolute error. The predictor selection algorithm is described in more detail in Nielsen et al. (2021). Note that Fox et al. (2017) raise concerns about the use of out-of-bag performance metrics in predictor selection, at least as a means for improving model accuracy without negatively impacting stability. Our primary purpose was instead to reduce model prediction time and to improve model spatial responsiveness. A cross-validation test could be used to evaluate the model accuracy of the reduced-predictor model vs. the full model on independent data. We did not perform that test.

2.5.1. Plausible willow habitat

We began by mapping plausible willow habitat, in order to limit over-mapping of willow arising from the subsequent imagery-based willow detection model. The process was designed to put a generous bounding extent around habitats where riparian and wetland willows might occur, and relied only on predictors descriptive of environmental setting (topography and climate). Positive training locations were provided by all current-era plots with willow presence and by VCMP plots with both willow presence and appropriate association calls (**Section 2.1.3.1**). Negative training was derived from upland EVMP aspen plots (**Section 2.1.3.3**) and by VCMP plots with inappropriate association calls.[15]

The data reduction process (i.e., the use of **caret** to reduce multicollinearity) resulted in keeping six of the 30 climate predictors and 17 of the 32 topography predictors. The RF-guided predictor selection process resulted in a model based on four climate predictors and nine topography predictors.[16] The selected predictors were used to create a RF classification model of 1001 trees, with each tree based on a training sample size for each class equal to the minimum number of training plots available for either class.[17] We estimated model error rates using 1000 bootstrap samples, each constructed by holding out one plot from the least common class and a proportional number from the most common class. The model was then predicted wall-to-wall at 3-meter resolution, and the output probabilities were saved for later use.

2.5.2. Image-based willow presence

We mapped willow presence using a model which relied only on image-based predictors.[18] Two runs were performed, one indicative of pre-fire conditions in 2019–20 and the other of post-fire conditions in 2021. The pre-fire run made use of NAIP imagery from 2019 and Sentinel-2 imagery from 2019 and 2020; the post-fire run substituted 2021 Sentinel-2 imagery.[19] Positive training locations were provided by current-era plots with willow presence, with the exception that plots sampled prior to 2021 were excluded from the post-fire run if they were mapped as disturbed in the 2020–21 interval. Negative training was provided by current-era willow and wetland plots that lacked willow, by

---

[15] **Table 2** summarizes the plots used as training data in the plausible habitat model.

[16] Climate: *ppt_jul*, *tdew_jan*, *vmin_jul*, *vmin_oct*. Topography: *cpl750*, *cpr750*, *dih_c*, *dih_r*, *dtw_c*, *rough270*, *rough90*, *tpma300*, *tpma7500*, *wet30*. See Nielsen et al. (2021) for descriptions of these predictors.

[17] When the classes to be predicted are not represented evenly in the training data, the more common class has a tendency to be modeled with greater accuracy than the other. This effect can be alleviated by downsampling the more common class (see Evans and Cushman 2009). The same technique was used earlier during the predictor selection phase.

[18] The presence model was created independently of the habitat model; the two model outputs were combined in the subsequent step.

[19] Despite the 2019 NAIP imagery no longer representing current conditions for areas disturbed in late 2020, we found that incorporating it in 2021 modeling resulted in slightly better model performance in these locations. It is possible that information regarding pre-fire stand conditions was in some way helpful in diagnosing willow survival. The 2019 NAIP imagery was **not** used in 2021 attributes mapping, only for predicting willow presence.

riparian EVMP aspen plots with sufficient aspen density (**Section 2.1.3.3**), by photo-interpreted plots in various locations that clearly lacked willow (**Section 2.1.4.1**),[20] and by VCMP plots which lay in areas mapped with 50% or greater probability as plausible willow habitat (**Section 2.5.1**) but which lacked willows in 2002–04.[21]

For the pre-fire run, data reduction kept 108 of the 344 NAIP predictors and 11 of the 53 Sentinel-2 predictors. The RF-guided predictor selection process resulted in models based on 18 NAIP predictors and one Sentinel-2 predictor.[22] For the post-fire run, data reduction kept 92 of the 344 NAIP predictors and 20 of the 58 Sentinel-2 predictors.[23] The RF-guided predictor selection process resulted in models based on 17 NAIP predictors and five Sentinel-2 predictors.[24] The model creation and error rate estimation tasks were done as in **Section 2.5.1**.

2.5.3. Fused willow presence

We combined the outputs of the setting-based plausible habitat model and the image-based willow presence model to create final willow presence maps for summer 2020 and summer 2021. We calculated the probability of willow presence, p_{pres}, as the geometric mean of the probability outputs of the habitat and image-based presence models:

$$p_{pres} = \sqrt{p_{habitat}\, p_{pres\_img}}$$

[20] A number of photo-interpreted plots were created in areas that were severely burned in late 2020, for use as willow absence data for the 2021 run.

[21] **Table 2** summarizes the plots used as training data in the image-based presence model. VCMP plots were used only to provide willow absence data, based on the assumption that willow has declined in many areas since 2002–04, but has increased in very few places. VCMP plots which lay in areas outside mapped plausible willow habitat were not used as negative training to avoid diverting the presence model from its focus on distinguishing presence from absence within plausible habitat. There is a risk in including negatives from VCMP plots but positives only from willow and wetland plots, in that the presence model may show bias against detection of willows in habitat that lay outside the EVMP willow sample universe. The use of only image-based predictors in the presence model effectively counters this risk, since the model has no setting-based predictors available with which to act on such a bias.

[22] NAIP: *d6c*, *ddc*, *e4c*, *g1_md*, *ga_13*, *gb_26*, *nc_9e*, *rc_13*, *u1_mx*, *u1b*, *uc_26*, *vb_26*, *vb_6d*, *w1c*, *wb_13*, *wb_26*, *x1_mx*, *y1_mx*. Sentinel-2: *ndgbp* (July 2020). See Nielsen et al. (2021) for descriptions of these predictors.

[23] Fewer total Sentinel-2 predictors were available for the 2020 run because the September 2019 Sentinel-2 blue reflectance band was impacted by smoke or haze. We dropped predictors which relied on this band from that image.

[24] NAIP: *b1_mx*, *d2c*, *e2c*, *e6c*, *gc_13*, *gc_cf*, *n1_md*, *r2c*, *rb_13*, *rb_26*, *ub_13*, *v1_md*, *v1b*, *vb_39*, *vc_4c*, *w1b*, *x1_mx*. Sentinel-2: *grn* (Aug. 2021); *ndsi*, *nir*, *tcb*, *tcw* (Sep. 2021). See Nielsen et al. (2021) for descriptions of these predictors.

A 3x3-cell focal mean was used to smooth the resulting 3-meter resolution presence probability. We treated willow as present on pixels with smoothed $p_{pres} \geq 0.5$.[25]

2.5.4. Willow cover, height and leaf area index

We used RF regression models to map continuous-valued willow attributes, including stand canopy cover, height and LAI.[26] These models made use of both setting-based and image-based predictor sets. Again, two runs were performed, to represent pre-fire and post-fire conditions. The pre-fire run used 2019 NAIP imagery and Sentinel-2 imagery from 2019 and 2020, while the post-fire run used only 2021 Sentinel-2 imagery.

Training data came from current-era plots with willow present and non-zero values for all attributes. The cover, height and LAI estimates were derived using the methods described in **Section 2.2**. To provide training data at very low values of the willow attributes, we used current-era plots which lay in areas where willow was mapped as present (**Section 2.5.3**) but in which no willow was found.[27] We treated these plots as having minimal cover (0.01%), height (0.01 cm), and LAI (0.01). Plots sampled prior to 2021 were excluded from the post-fire run if they were mapped as disturbed in the 2020–21 interval.[28]

For the pre-fire run, in addition to the 108 NAIP predictors and 11 Sentinel-2 predictors available to predictor selection for the presence model, data reduction kept four of the 30 climate predictors and 21 of the 32 topography predictors. For the post-fire run, in addition to the 92 NAIP predictors and 20 Sentinel-2 predictors available to predictor selection for the presence model, data reduction kept four of the climate predictors and 20 of the topography predictors. The predictors chosen during the predictor selection process differed for the different attributes models, discussed below. For each attribute, the selected predictors were used to create a RF regression model of 1001 trees.

Over-prediction of low values and under-prediction of high values is typical of machine learning regression modeling and can be reduced in several ways (Zhang and Lu 2011). We used Model 2 (reduced major axis) regression to compensate for model bias toward the mean at very low and very high values of the attribute variable (see Belitz and Stackelberg 2021). We derived a bias-correcting slope and intercept by regressing the input attribute values of all plots on the bootstrapped attribute predictions. After wall-to-wall prediction of each attribute, the slope and intercept derived from the bias-correction procedure was applied to all pixel predictions.

---

[25] We used the default threshold of 0.5 because both constituent models—the habitat and imagery-based presence model—had well-balanced training data, and it was not clear that the costs of false positives and false negatives should differ for our application.

[26] We considered the use of artificial neural networks for these tasks but lacked sufficient field data to parameterize them.

[27] This step is similar to the process used for VCMP plots in **Section 2.5.2**. By only using willow absence plots where willow was mapped as present, we exclude the obvious cases and focus the model on the real task.

[28] **Table 2** summarizes the plots used as training data in each of the attributes models.

For all attributes models, two raster outputs were produced. In output A, all pixels where willows were predicted as present in **Section 2.5.3** received an attribute prediction of at least 0.001 (%, cm, or unitless LAI). If the bias correction resulted in a negative value, the prediction was raised to 0.001. In output A, willow absence pixels are indicated by the valid raster value of zero. In output B, if bias correction resulted in a negative value, the prediction was raised to zero. In this output, willow absence pixels are indicated by a nodata (invalid) raster value.

2.5.4.1. Willow canopy cover

For the pre-fire run, the RF-guided predictor selection process resulted in models based on 15 NAIP predictors, eight topography predictors, five Sentinel-2 predictors, and three climate predictors.[29] For the post-fire run, the RF-guided predictor selection process resulted in models based on five Sentinel-2 predictors, five topography predictors, and one climate predictor.[30] Maps were generated using only these predictors.

2.5.4.2. Willow canopy height

For the pre-fire run, the RF-guided predictor selection process resulted in models based on 20 NAIP predictors, nine topography predictors, three Sentinel-2 predictors, and two climate predictors.[31] For the post-fire run, the RF-guided predictor selection process resulted in models based on 11 Sentinel-2 predictors, 11 topography predictors, and four climate predictors.[32] Maps were generated using only these predictors.

2.5.4.3. Willow leaf area index

For the pre-fire run, the RF-guided predictor selection process resulted in models based on six NAIP predictors, four topography predictors, and four climate predictors.[33] For the post-fire run, the RF-guided predictor selection process resulted in models based on seven topography predictors, five Sentinel-2 predictors, and two climate predictors.[34] Maps were generated using only these predictors.

---

[29] NAIP: *d3c*, *e2c*, *e4c*, *e6c*, *g1_md*, *ga_26*, *n1b*, *nc_6d*, *r1c*, *u1b*, *uc_13*, *ufb*, *wa_cf*, *x1_mx*, *y1_mx*. Topography: *be10*, *cold1500*, *cpl750*, *cpr750*, *dih_r*, *dtw_c*, *dtw_r*, *tpmi7500*. Sentinel-2: *grn*, *ndgbp*, *ndsi*, *sw1* (July 2020); *grn* (Sep. 2019). Climate: *tmin_avg*, *vmax_apr*, *vmin_oct*. See Nielsen et al. (2021) for descriptions of these predictors.

[30] Sentinel-2: *blu*, *ndgrp*, *ndsip* (Aug. 2021); *blu*, *ndmi* (Sep. 2021). Topography: *be10*, *cold1500*, *dih_c*, *dih_r*, *rough810*. Climate: *tdew_jan*. See Nielsen et al. (2021) for descriptions of these predictors.

[31] NAIP: *d6c*, *e2c*, *e3c*, *e4c*, *g1_md*, *ga_13*, *ga_26*, *gb_13*, *gb_9e*, *gdc*, *nc_6d*, *r1c*, *rc_13*, *rc_cf*, *u1b*, *uc_13*, *vb_4c*, *vc_6d*, *w1c*, *x1_mx*. Topography: *be10*, *cold1500*, *cpr150*, *cpr30*, *cpr750*, *dih_r*, *dtw_r*, *rough810*, *tpma1500*. Sentinel-2: *grn*, *ndsi* (July 2020); *ndgrp* (Sep. 2019). Climate: *tmin_avg*, *vmax_apr*.

[32] Sentinel-2: *grn*, *ndgbp*, *ndgrp*, *ndmi*, *ndsip*, *ndsw* (Aug. 2021); *ndgb*, *ndgbp*, *ndmi*, *ndsi*, *tcw* (Sep. 2021). Topography: *be10*, *cold1500*, *cold300*, *cpr150*, *dih_c*, *dih_r*, *rough810*, *tpma1500*, *tpma300*, *tpma7500*, *tpmi7500*. Climate: *ppt_jul*, *tdew_jan*, *tmin_avg*, *vmin_oct*.

[33] NAIP: *e2c*, *g1_md*, *ga_26*, *r1c*, *ufb*, *x1_mx*. Topography: *be10*, *dtw_c*, *dtw_r*, *tpmi7500*. Climate: *ppt_apr*, *tmin_avg*, *vmax_apr*, *vmin_oct*.

[34] Topography: *cold1500*, *cold300*, *cpr750*, *dih_c*, *dih_r*, *rough810*, *tpma1500*. Sentinel-2: *blu*, *ndgrp*, *ndsip* (Aug. 2021); *blu*, *ndmi* (Sep. 2021). Climate: *tdew_jan*, *vmin_oct*.

2.5.5. Fusion of runs

The final maps of willow cover, height, and LAI were produced by combining the more accurate pre-fire model results[35] with the post-fire model results. The pre-fire results were used everywhere except in locations which were mapped as disturbed in the 2020–21 time interval.

3. Results and discussion

3.1. Model accuracy

3.1.1. Habitat model

The bootstrapped error assessment indicated an overall error rate of 11.9% in modeling plausible willow habitat. The error was well-balanced, with plots labeled as implausible habitat predicted incorrectly at a rate of 11.4%, and plausible habitat plots predicted incorrectly 13.0% of the time.

3.1.2. Imagery-based presence models

The bootstrapped error assessment indicated an overall error rate of 19.3% in modeling pre-fire presence of willows, even at the smallest amounts. The error was well-balanced, with willow absence plots predicted incorrectly at a rate of 17.6%, and willow presence plots predicted incorrectly 20.9% of the time. The overall error rate in modeling post-fire willow presence was 15.1%. The error rate for willow absence plots, at 17.8%, was similar to the pre-fire model, but significantly less omission error was observed. Only 12.4% of willow presence plots were predicted incorrectly. The different results are likely not particularly meaningful, as they probably result from the inclusion of a number of heavily scorched photo-interpreted willow absence plots in the training dataset.

3.1.3. Continuous willow attribute models

The results of the model error assessments for the pre- and post-fire runs for each of the attributes are shown in **Table 7**. The post-fire models, lacking predictors based on aerial imagery, had higher error rates than the pre-fire models. The post-fire results are only used in locations where disturbance occurred between summer 2020 and summer 2021. Model error rates were evaluated over bootstrap-aggregated samples independent from the training data.

Table 7. Bootstrap-aggregated model root-mean-square error (RMSE) and R^2 for the three attributes models for each of the modeled time periods.

Attribute	Time period	Model RMSE	Model R^2
Canopy cover	pre-fire (2019–20)	19.2%	0.495
	post-fire (2021)	26.3%	0.345
Canopy height	pre-fire (2019–20)	48.9 cm	0.560
	post-fire (2021)	55.0 cm	0.469
Leaf area index	pre-fire (2019–20)	1.56	0.520
	post-fire (2021)	1.94	0.368

[35] The pre-fire models were more accurate (**Section 3.1**) because of their inclusion of predictors derived from the 2019 NAIP.

3.2. Maps

Resulting maps for plausible willow habitat, fused willow presence, canopy height and LAI are shown for the full park in **Figures 12–15**.[36] **Figures 16–19** have closer views of the KV (LAI), some east-side valleys (LAI and height), and a full-resolution LAI image from Horseshoe Park.

[36] Willow canopy cover is not shown because at this scale it closely resembles LAI.

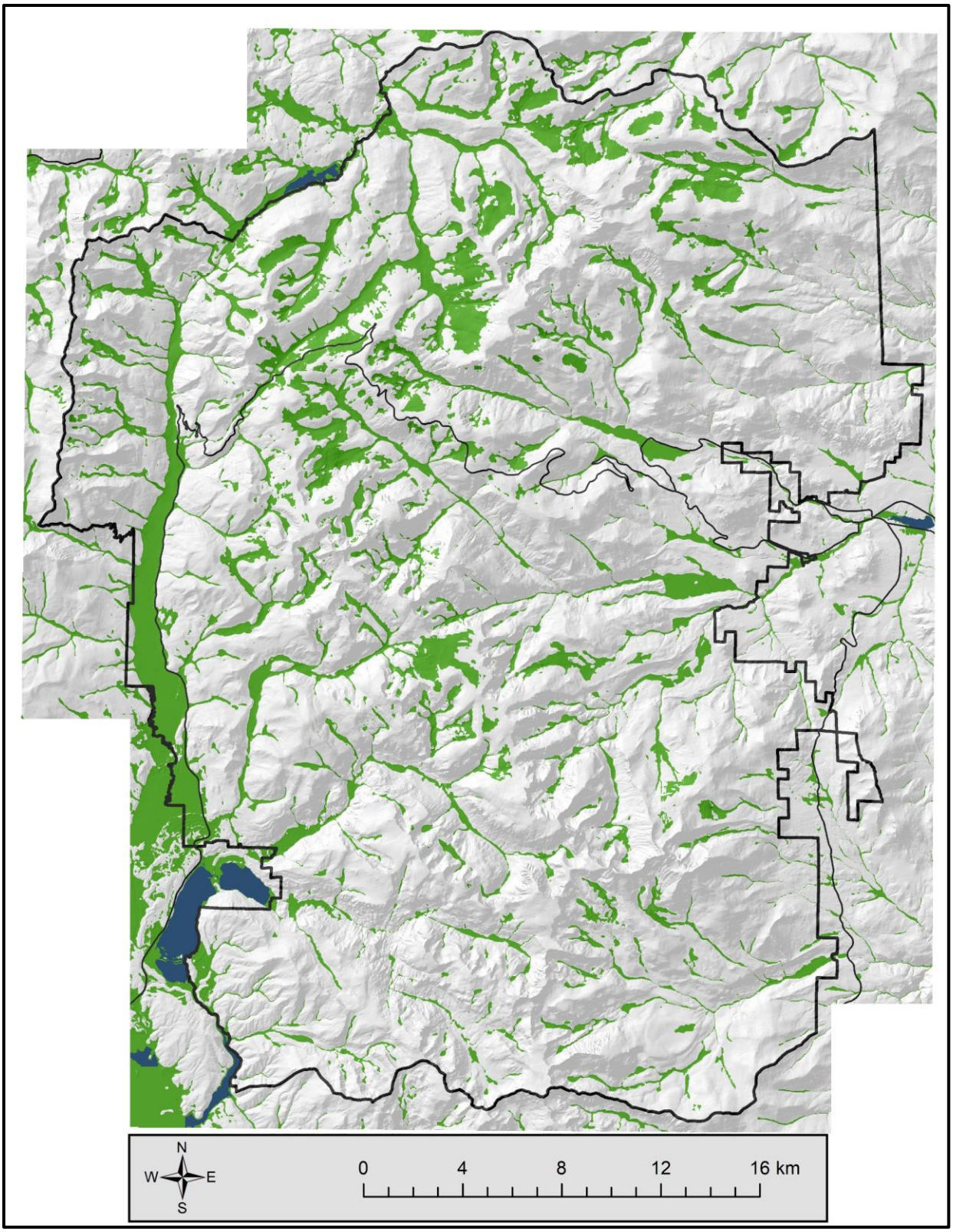

Figure 12. Plausible willow habitat is shown in green. Much of this area would not support willow stands; individual willow plants may be restricted to suitable microsites.

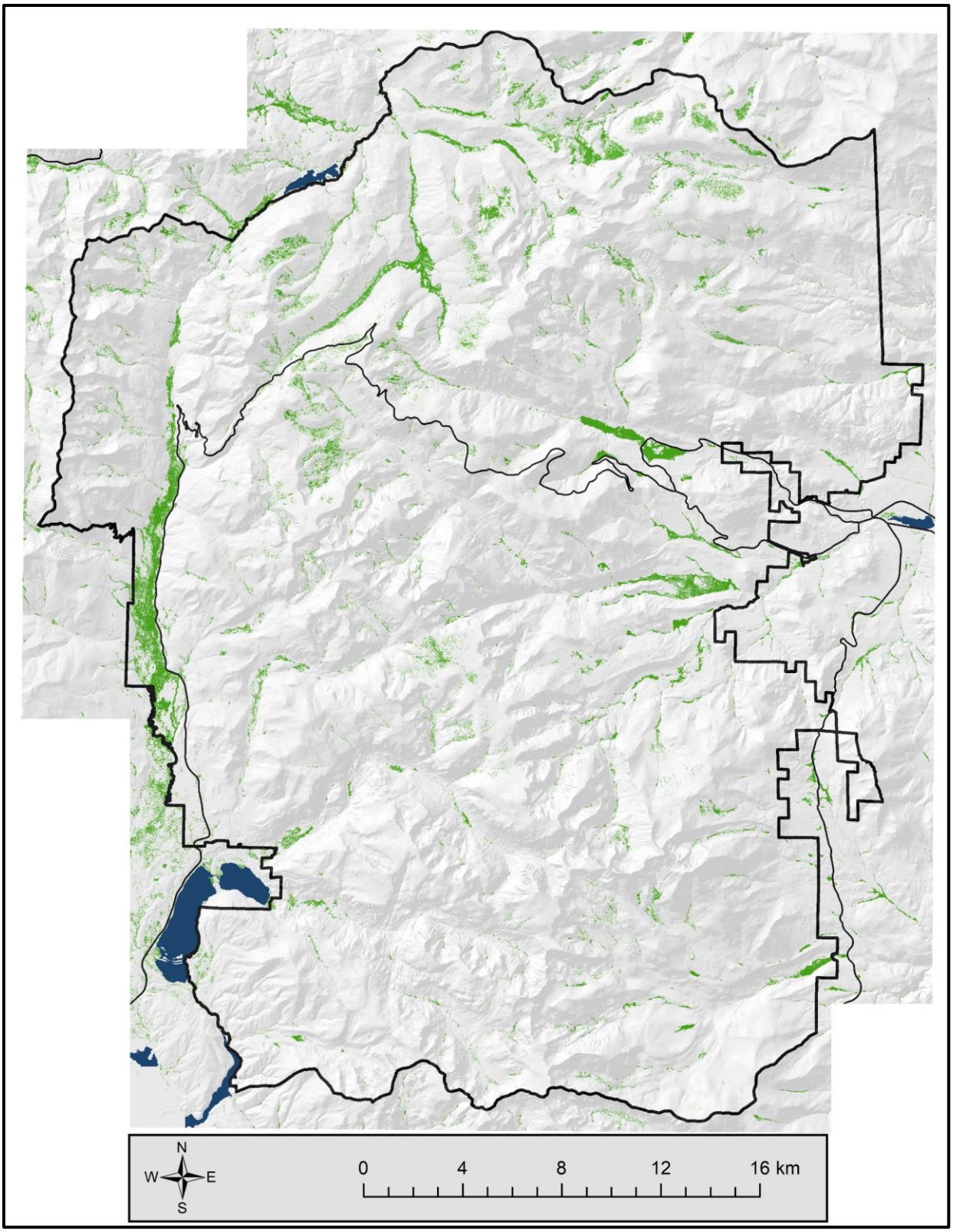

Figure 13. Summer 2021 willow presence is shown in green. Many mapped willow occurrences may not represent stands but rather individual willow plants restricted to suitable microsites.

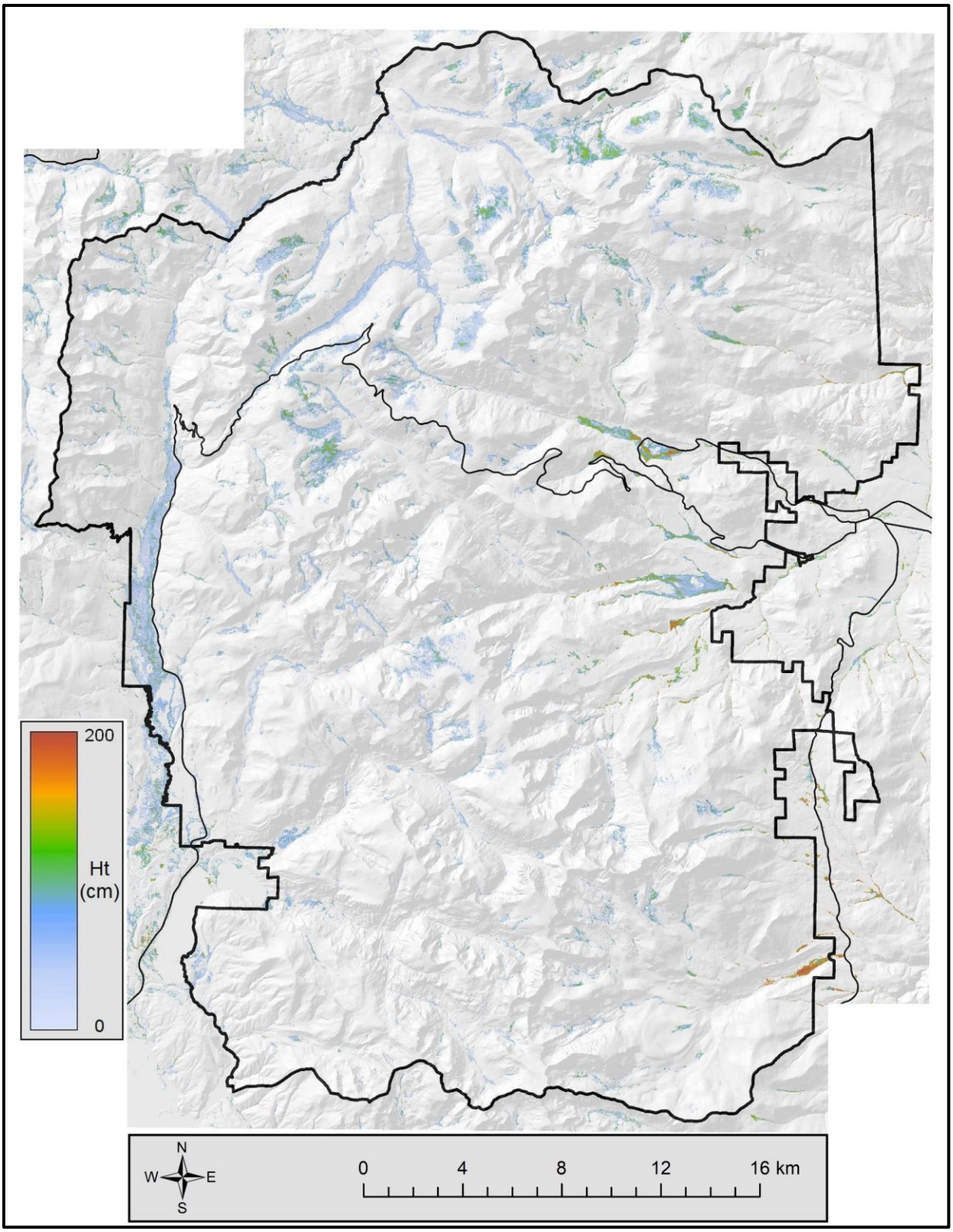

Figure 14. Summer 2021 willow canopy height.

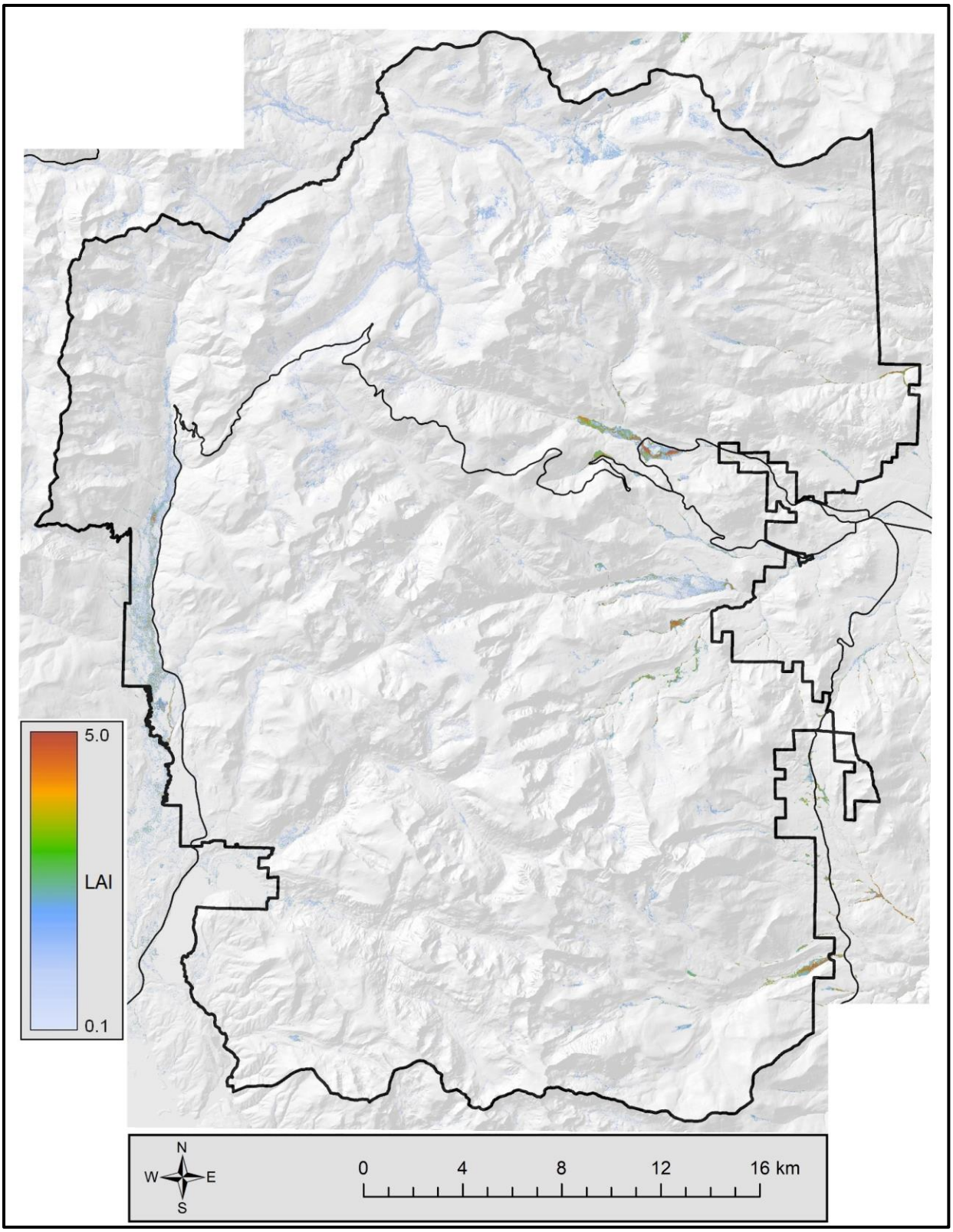

Figure 15. Summer 2021 willow canopy leaf area index.

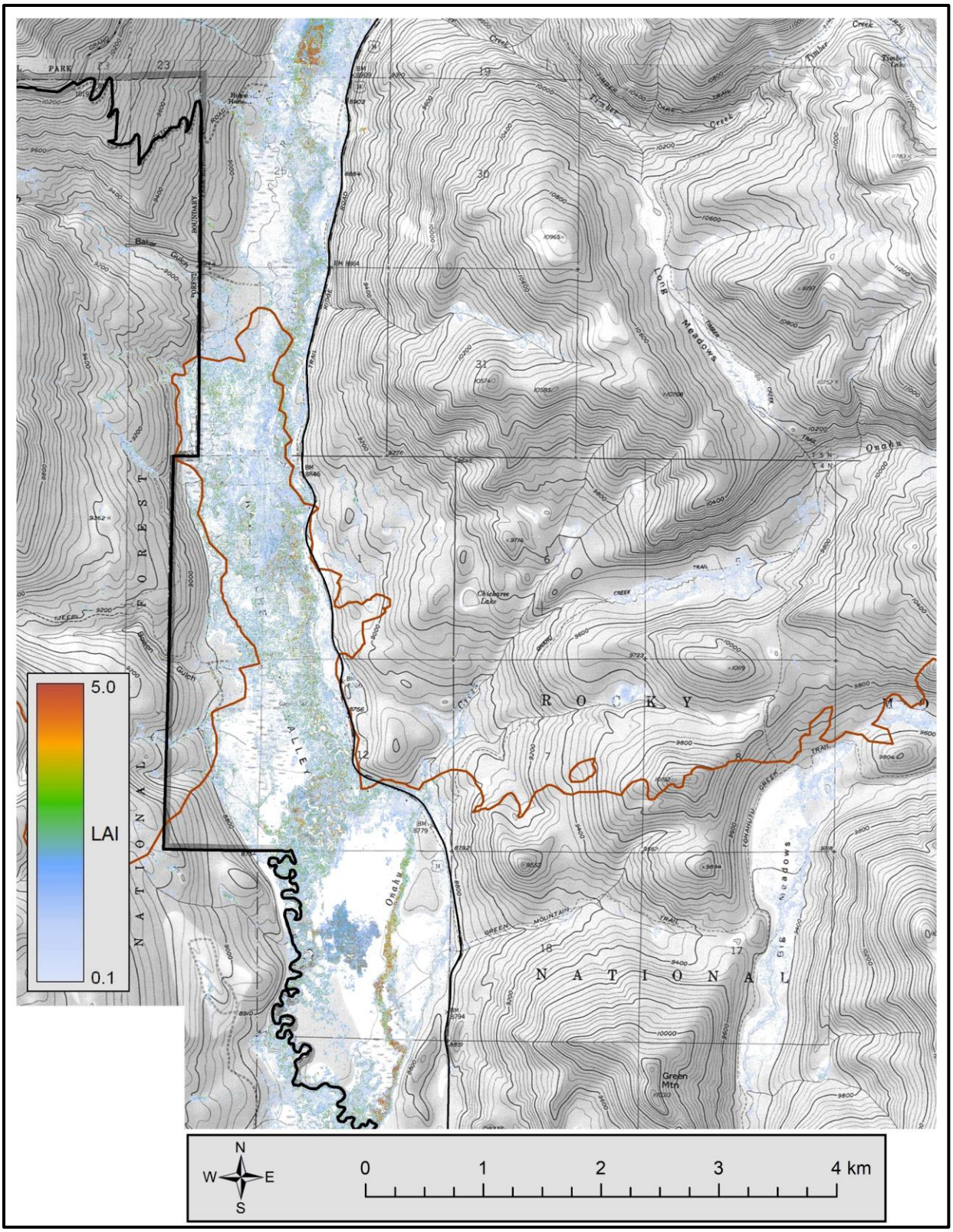

Figure 16. Summer 2021 willow canopy leaf area index in the KV. The 2020 fire boundaries are shown. Note the area of high LAI in the exclosure at the north end of the visible area.

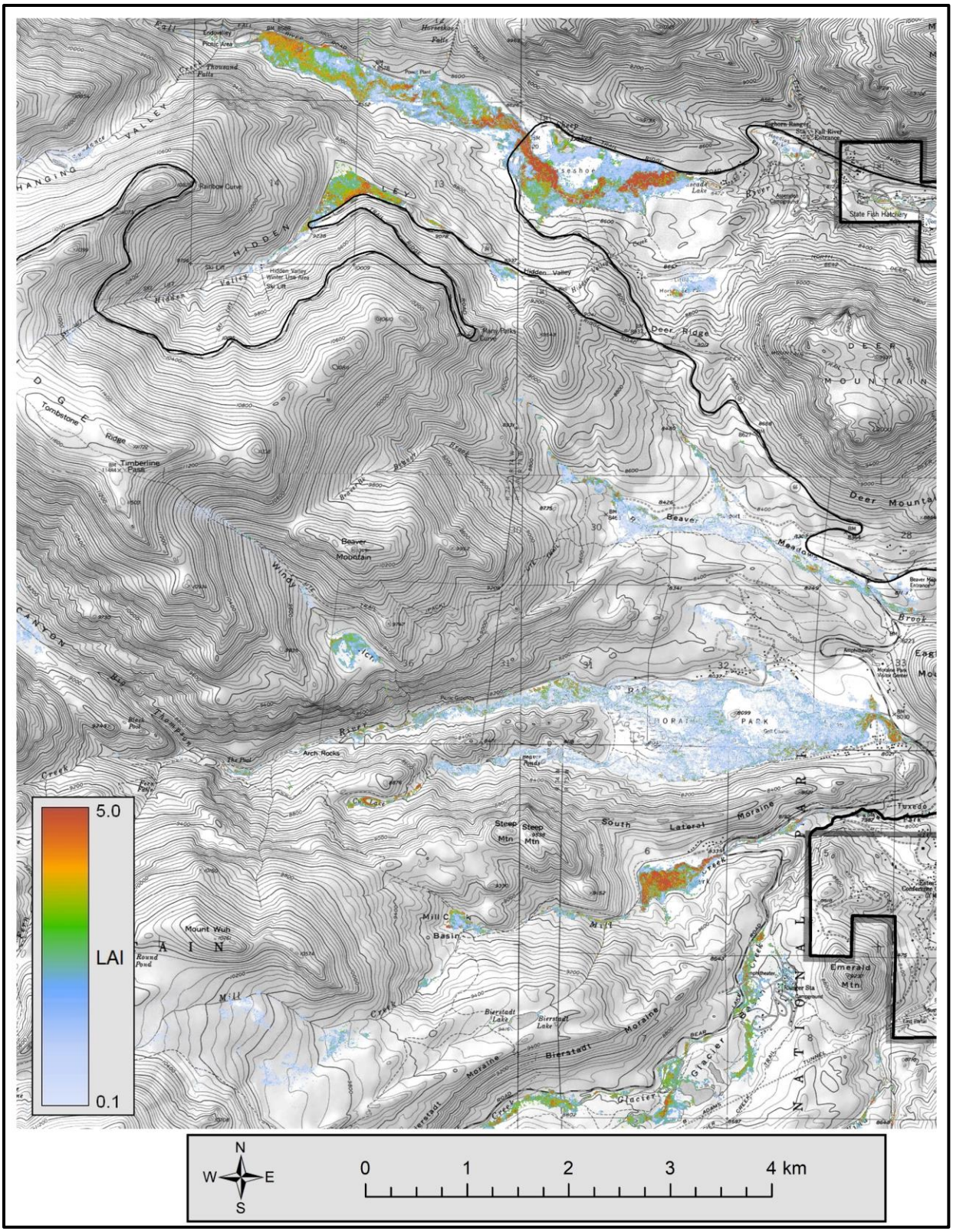

Figure 17. Summer 2021 willow canopy leaf area index in some of the east side valleys.

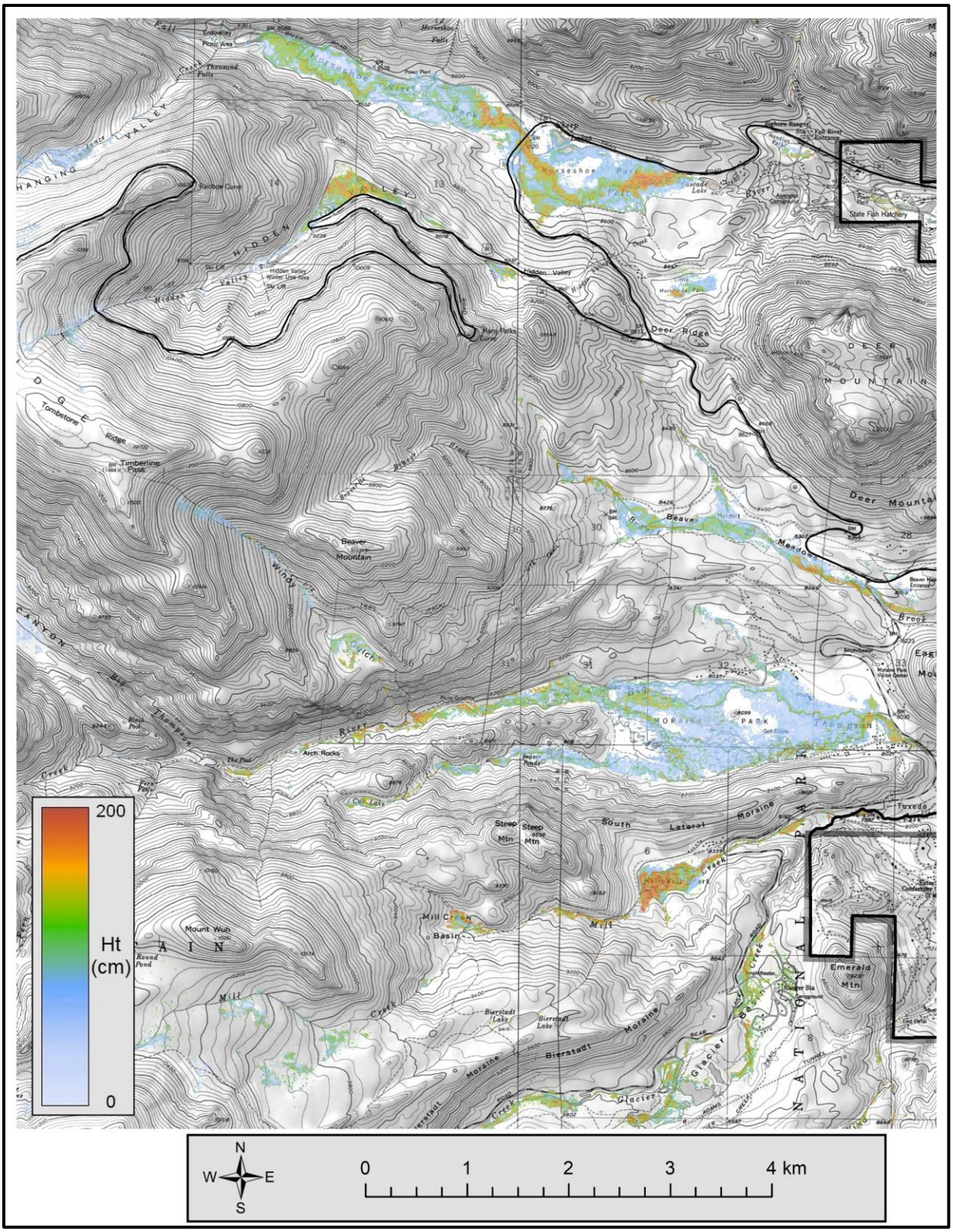

Figure 18. Summer 2021 willow canopy height in some of the east side valleys.

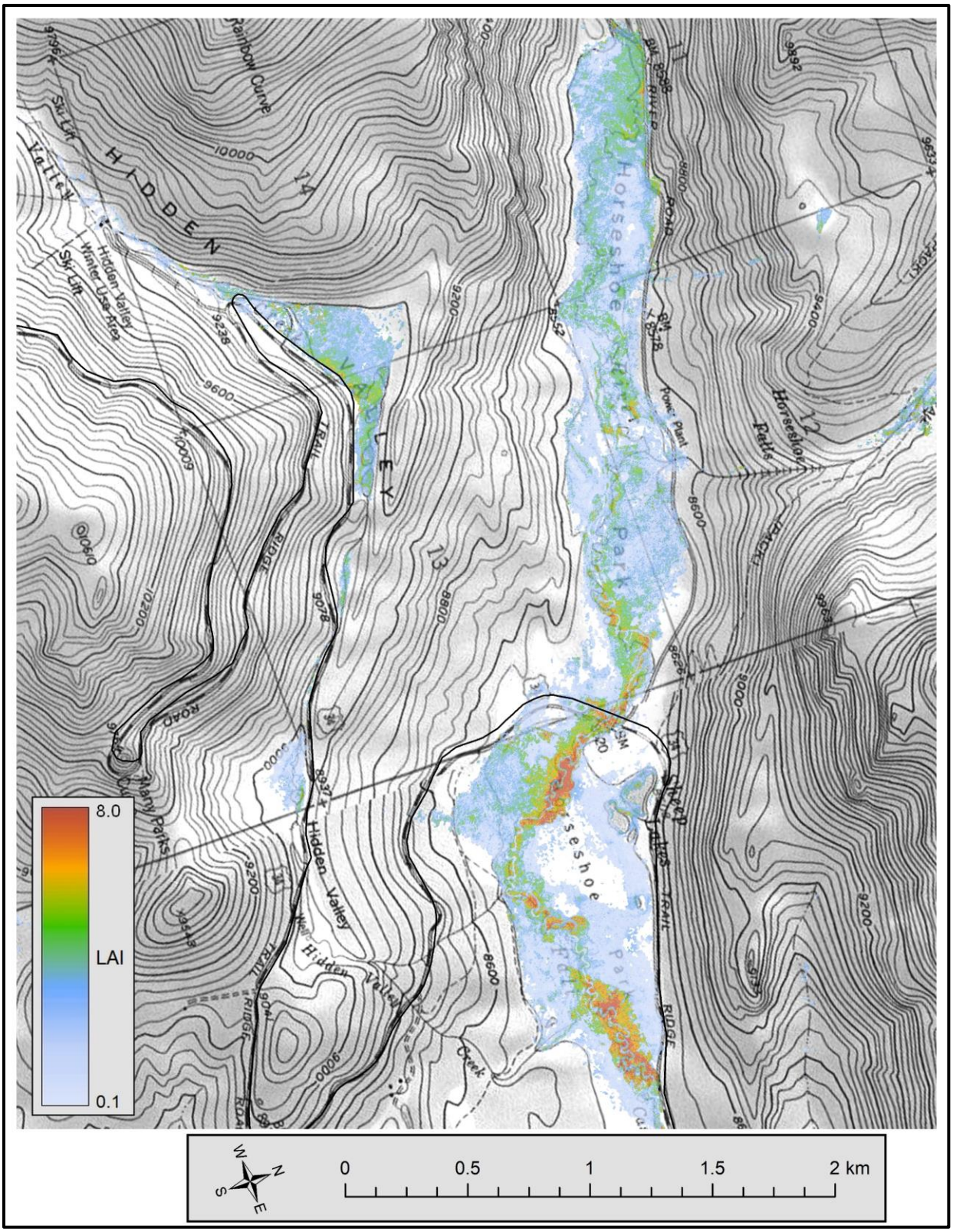

Figure 19. Summer 2021 willow canopy leaf area index in Horseshoe Park. Note the color scale is changed in this image; Horseshoe Park includes areas mapped with LAI as high as 12.2.

3.3. Leaf area summaries

Riparian and wetland willows were mapped as present[37] on 5.45% of the park's 1079.9 km^2. Where willow was mapped as present, the mean mapped willow leaf area index was 0.694. Although this LAI would represent a very sparse willow stand, most of these mapped occurrences likely represent vegetation types where willow is not dominant but only a component. We did not attempt to distinguish willow-dominated stands from other vegetation in this project.

Table 8 summarizes the mean mapped willow LAI (using output B) across the different moose management areas (MMAs) within the park.[38] Areas inside and outside exclosure fencing are separated. Totaled across MMAs that have exclosures, the LAI of willows within exclosures exceeds that of willows outside exclosures by a factor of 3.6. The MMAs with the highest mean willow LAI are Cow Creek, Hollowell Park and Wild Basin. However, willow LAI within fenced areas in Horseshoe Park, the Kawuneeche Valley, and Endovalley rivals or exceeds those areas.

Table 8. Mean willow leaf area index by moose management area, separated by areas inside and outside of exclosure fencing. Mean values apply to the entire summary unit, not only the portion where willow is present.

			Mean willow leaf area index		
Moose management area	**Area (km^2)**	**% of area with exclosures**	**Outside exclosures**	**Inside exclosures**	**Entire area**
Big Meadows	1.360	0.00%	0.080	–	0.080
Chapin Creek–Cache La Poudre	6.194	0.00%	0.191	–	0.191
Cow Creek	0.138	0.00%	3.350	–	3.350
Endovalley	1.410	8.89%	1.487	2.379	1.566
Hollowell Park	0.226	0.00%	3.043	–	3.043
Horseshoe Park	1.393	14.02%	0.985	4.575	1.488
Kawuneeche Valley	14.253	0.51%	0.529	2.865	0.541
Long Meadow	0.570	0.00%	0.032	–	0.032
Moraine Park	3.617	13.08%	0.355	1.266	0.474
North Inlet	2.212	0.00%	0.131	–	0.131
Upper Beaver Meadows	0.964	20.79%	0.282	1.075	0.447
Wild Basin	0.697	0.00%	2.249	–	2.249
All management areas	33.032	3.2%	0.508	2.076	0.559
All management areas with exclosures	21.636	4.9%	0.579	2.076	0.653

[37] At 3-meter pixel scale, using non-zero values of output B to represent willow presence.

[38] Note that in both **Table 8** and **Table 9**, in keeping with the focus of this work on producing cumulative totals, the mean LAI is given with reference to the total area within the summary unit, not with reference only to areas where willow is present (as presented in the first paragraph of **Section 3.3**). Map users can create LAI summaries with reference to willow presence by summarizing only over areas where LAI output B has values greater than zero.

Table 9 summarizes mapped willow LAI across several other areas of interest: modeled moose habitat and non-habitat within a moose count sample frame (Hobbs and Abouelezz 2023), and across the full extent of Rocky Mountain National Park.

Table 9. Mean willow leaf area index summarized with respect to modeled moose habitat status, and over the full park. Areas inside and outside of exclosure fencing are separated in each category. Mean values apply to the entire summary unit, not only the portion where willow is present.

			Mean willow leaf area index		
Summary area	Area (km^2)	% of area with exclosures	Outside exclosures	Inside exclosures	Entire area
Modeled habitat in sample frame	221.631	0.33%	0.093	2.196	0.100
Modeled non-habitat in sample frame	465.886	0.04%	0.015	1.622	0.016
Full park	1079.900	0.11%	0.036	1.997	0.038

3.4. Assessment against independent estimates

We assessed the realism of our results by comparing them to annual biomass production estimates made by Stumph (2005). In 2003–04, Stumph sampled willow species, canopy cover and height along transects at 33 sites in the Colorado River drainage of the park. He used this structural data to estimate average canopy volume by species at riparian willow communities in this region. The spatial extent of these communities was mapped from aerial photos, and the dry mass per unit canopy volume was estimated by clipping, drying and weighing all leaves from a sample of willow plants, none more than one meter in height.[39] Stumph estimated an annual willow biomass production of 184,128 kg across 4.579 km^2 of willow communities within the KV.

We excerpted the SHRUB–RIPARIAN–CROSS ZONE < 9600 FT map unit within the elevation range described by Stumph (2005) from the Salas et al. (2005) vegetation map, resulting in a summary zone of 4.257 km^2 which likely corresponds reasonably closely to Stumph's KV summary. Across this zone a total of 3.828 km^2 of willow leaf area was mapped. To convert mapped leaf area to corresponding leaf biomass, we used a specific leaf area (SLA) estimate of 14.3 m^2/kg, derived by averaging the estimates given for shade leaves from three plantation willow clones (see Table 2, Merilo et al. 2006),[40] resulting in a leaf biomass estimate of 267,736 kg.

Given the heavy dependence of SLA on depth in canopy (see Figure 1, Merilo et al. 2004), it is possible a higher SLA should be used to better correspond to Stumph's biomass sampling method. This would bring the biomass estimates into closer agreement. At any rate, given the degree of uncertainty in both estimates, it is encouraging that they are in the same order of magnitude, although

[39] Note that Stumph (2005) refers to "the poor state of some willow communities" in justifying the canopy sampling approach used. Significant decline had apparently occurred already by this time.

[40] Estimates were made for the species *Salix viminalis* and *S. dasyclados*, which are broadly similar in morphology and habitat to montane willow species in the park. We used the estimates from control (unfertilized) sites. We used the shade-leaf estimates to correspond more closely to the near-ground leaves sampled by Stumph (2005).

of course we expect to see some further decline in willows in the KV since the time of Stumph's work.

3.5. Guidelines for map use

Output A may be preferable for attribute map graphics. In these layers, it is possible to distinguish between pixels where willow was modeled as absent and pixels outside the modeling area. Output B may be preferable for tabular summaries, since the arbitrary minimum value assigned in output A to pixels with willow modeled as present but at vanishingly small amounts may sum to substantial amounts over many pixels.

The maps will be most reliable for relative comparison of areas with differing canopy cover, canopy height, and LAI. The calibration of the quantitative models to absolute values of these attributes was a more uncertain process, and was limited by the number, geographic representativeness and reliability of the field training data. No effort was spared in making the best use possible of all available field data, but ground-truth data availability remains a major limiting factor. Allometric conversions of leaf area index to annual biomass production are possible, but should be undertaken carefully. They may introduce a substantial additional element of uncertainty into the results.

3.6. Potential for map improvement

In constructing the LPI protocol, we attempted to balance the need for precise estimates at each site with that for a reasonably large and geographically diverse collection of plots. To address this tradeoff, we reduced the LPI sample density to just 16 point-intercept samples per plot.[41] It appears that this achieved our goals, because the derived relationships between cover, height and LAI are plausible, we obtained enough plots to support the modeling, and the modeling results themselves appear plausible. However, the significant resulting sampling error contributes to substantial uncertainty in the calibration of the LAI model to absolute quantities. Also, bias may result from the uneven geographic spread of the LPI plots used to generate the relationship connecting cover and height to LAI, and the small number of LPI plots collected—particularly for low-elevation species—may also weaken the reliability of that relationship.

The most obvious fix for the above issues is to dedicate additional field effort specifically to increasing the number and geographic representativeness of plots with measured leaf area, while simultaneously either increasing the number of point-intercept samples (using the current LPI protocol) or developing some alternative method for field estimation of LAI. First, though, it is worth considering whether it may be possible to circumvent the need for leaf area field estimates by locating or developing relationships that allow reasonable estimation of annual production from canopy cover and maximum plant height measurements. We are skeptical of that possibility,

[41] The clumped patterns frequently seen in willow canopy add to the uncertainty resulting from the small sample. In addition, changes in leaf orientation angle can make a large difference in LAI estimates using the LPI method. Crews were initially asked to estimate the angle from the horizontal of each leaf hit, but to reduce the time requirements we instead visually estimated the overall average leaf angle for each willow species present.

primarily due to a concern that the variable impacts of browse damage and other dieback will alter and/or weaken relationships between those attributes and biomass production, and the relationships would likely be inconsistent even within the park. Furthermore, live canopy cover and live stem height themselves may become more difficult to estimate consistently in the field under conditions of crown dieback.

Given the likely difficulty of relying on allometric relationships to approximate annual production in variously disturbed willow stands, we recommend adding some form of leaf area estimation to willow field sampling protocols. The LPI protocol developed for this project might be used for this purpose, though we recommend two main modifications: (1) increasing the number of point-intercept samples on the LPI transect to reduce the sampling error to a reasonable amount, and (2) estimation of average leaf angle at each point.

Another option might be to use some sort of volumetric sample; for example, by counting the number of leaves within a visualized cylinder surrounding each vertical cross-section. This would provide a larger sample, and the leaf angle would no longer be a disruptive variable. The radius of the cylinder could vary by plot depending on canopy density, although it should remain consistent within any plot. There are certainly other possibilities.[42]

Whatever method is used to estimate leaf area, visual estimates of willow live canopy cover should be made for all species, not only the most abundant. Try to make these estimates to the nearest one percent, without spending time trying to do the impossible. The important thing is not to leave obvious information on the table. High precision of these estimates is most important, and also most feasible, when canopy cover is low (especially at 5% or less).

The most efficient and reliable approach to estimating LAI is likely to rely both on visual estimates (which are more robust for clumped canopies) and on mechanistic sampling (because visual estimation of leaf area is inherently a very difficult task). For example, mechanistic leaf area sampling could be confined only to the portions of a plot where willow canopy is present, and the leaf area estimates could then be prorated by a visual cover estimate. Finally, in order to more reliably convert estimated leaf area to annual leaf biomass production, it seems well worth investing some effort in pulling leaves[43] and working up good species-specific estimates of specific leaf area.

---

[42] For example, various expensive devices have been created which attempt to estimate leaf area based on light flux through a vegetation canopy, or using an upward-facing camera. These are finicky, time-consuming, and seem unlikely to be well-suited to this application, but you might investigate.

[43] Leaves sampled for this purpose should be pulled from across the vertical cross-section of the willow canopy, because SLA varies substantially along this axis (see Merilo et al. 2004).

Literature Cited

Belitz, K. and P.E. Stackelberg. 2021. Evaluation of six methods for correcting bias in estimates from ensemble tree machine learning regression models. Environmental Modelling & Software 139: 105006. Online: https://www.sciencedirect.com/science/article/pii/S1364815221000499.

Bivand, R., T. Keitt and B. Rowlingson. 2014. R package 'rgdal' version 0.8-16. Online: https://cran.r-project.org/web/packages/rgdal/index.html.

Breiman, L. 2001. Random forests. Machine Learning 45:5–32.

Conrad, O., B. Bechtel, M. Bock, H. Dietrich, E. Fischer, L. Gerlitz, J. Wehberg, V. Wichmann and J. Böhner. 2015. System for Automated Geoscientific Analyses (SAGA) version 2.1.4. Geoscientific Model Development 8:1991–2007.

Contento, T.E. 2021. Willow growth response to altered disturbance regimes in Rocky Mountain National Park: herbivory, water levels, and hay production. Masters Thesis, Colorado State University. Online: https://mountainscholar.org/bitstream/handle/10217/234199/Contento_colostate_0053N_16953.pdf.

Curran, P. J. 1983. Multispectral remote sensing for the estimation of green leaf area index. Philosophical Transactions of the Royal Society of London. Series A, Mathematical and Physical Sciences 309:257–270.

Cutler, D.R., T.C. Edwards, K.H. Beard, A. Cutler, K.T. Hess, J. Gibson and J.J. Lawler. 2007. Random forests for classification in ecology. Ecology 88:2783–2792.

Dungan, J.D. and R.G. Wright. 2005. Summer diet composition of moose in Rocky Mountain National Park, Colorado. Alces 41:139–146.

Evans, J.S. and S.A. Cushman. 2009. Gradient modeling of conifer species using random forests. Landscape Ecology 24:673–683.

Fox, E.W., R.A. Hill, S.G. Leibowitz, A.R. Olsen, D.J. Thornbrugh and M.H. Weber. 2017. Assessing the accuracy and stability of variable selection methods for random forest modeling in ecology. Environmental Monitoring and Assessment 189: 316. Online: https://doi.org/10.1007/s10661-017-6025-0.

Google. 2021. Google Earth Engine. Online: https://earthengine.google.com.

Hijmans, R.J. 2018. R package 'raster': geographic data analysis and modeling, version 2.8-4. Online: https://cran.r-project.org/package=raster.

Hobbs, N.T and H.G. Abouelezz. 2023. Final report: models and data for predicting the abundance of moose and elk on the summer range in Rocky Mountain National Park. Task Agreement Number P17AC00863.

Kaczynski, K.M., D.J. Cooper and W.R. Jacobi. 2014. Interactions of sapsuckers and Cytospora canker can facilitate decline of riparian willows. Botany 92:485–493. Online: https://sites.warnercnr.colostate.edu/davidcooper/wp-content/uploads/sites/15/2017/02/2014Kaczynski-et-al.-Botany.pdf.

Kuhn, M. 2008. Building predictive models in R using the caret package. Journal of Statistical Software 28:1–26. Online: https://www.jstatsoft.org/article/view/v028i05.

Liaw, A. and M. Wiener. 2002. Classification and regression by randomForest. R News 2002:18–22. Online: https://cran.r-project.org/doc/Rnews/Rnews_2002-3.pdf. Code online: https://cran.r-project.org/package=randomForest.

Merilo, E., K. Heinsoo and A. Koppel. 2004. Estimation of leaf area index in a willow plantation. Proc. Estonian Acad. Sci. Biol. Ecol. 53:3–13. Online: https://www.digar.ee/arhiiv/et/download/146626.

Merilo, E. K. Heinsoo, O. Kull, I. Söderbergh, T. Lundmark and A. Koppel. 2006. Leaf photosynthetic properties in a willow (*Salix viminalis* and *Salix dasyclados*) plantation in response to fertilization. European Journal of Forest Research 125:93–100. Online: https://www.researchgate.net/publication/226059483_Leaf_photosynthetic_properties_in_a_willow_Salix_viminalis_and_Salix_dasyclados_plantation_in_response_to_fertilization.

Nielsen, E.M., C. Copass, R.L. Brunner and L.K. Wise. 2021. Olympic National Park vegetation classification and mapping project report. Natural Resource Report NPS/NCCN/NRR—2021/2255. National Park Service, Fort Collins, Colorado. Online: https://irma.nps.gov/DataStore/Reference/Profile/2286420.

Nielsen, E.M. and M.D. Noone. 2014. Tree cover mapping for assessing greater sage-grouse habitat in eastern Oregon. Report, 10 pp. Portland, OR: Portland State University and The Nature Conservancy.

PRISM Climate Group. 2021. PRISM climate data. Online: https://prism.oregonstate.edu.

R Development Core Team. 2020. R: a language and environment for statistical computing. R Foundation for Statistical Computing, Vienna, Austria. Online: https://www.r-project.org.

Salas, D., J. Stevens and K. Schulz. 2005. Rocky Mountain National Park, Colorado: 2001–2005 vegetation classification and mapping. Final report. Technical Memorandum 8260–05–02. Bureau of Reclamation, Denver, Colorado. Online: https://cnhp.colostate.edu/download/documents/2005/romorpt.pdf.

Schweiger, E.W., E. Gage, K.M. Haynes, D. Cooper, L. O'Gan and M. Britten. 2015. Rocky Mountain Network wetland ecological integrity monitoring protocol: Narrative, version 1.0. Natural Resource Report NPS/ROMN/NRR—2015/991. National Park Service, Fort Collins, Colorado. Online: https://irma.nps.gov/DataStore/Reference/Profile/2222993.

Stumph, B.P. 2005. The summer forage quality of willow communities and its influence on moose foraging ecology in Rocky Mountain National Park, Colorado. Masters Thesis, University of Idaho.

USDA NRCS. 2023. The PLANTS Database. National Plant Data Team, Greensboro, North Carolina. Online: https://plants.usda.gov/home.

USGS. 2021. 3D elevation program. Online: https://www.usgs.gov/3d-elevation-program.

Python Software Foundation. 2010. Python language reference, version 2.7. Online: http://www.python.org.

Zhang, G. and Y. Lu. 2011. Bias-corrected random forests in regression. Journal of Applied Statistics 39: 151-160. Online: http://dx.doi.org/10.1080/02664763.2011.578621.

Zeigenfuss, L., T. Johnson and Z. Wiebe. 2011. Monitoring plan for vegetation responses to elk management in Rocky Mountain National Park. U.S. Geological Survey Open-File Report 2011–1013. 85p. Online: https://pubs.usgs.gov/of/2011/1013/pdf/OF11-1013.pdf.

Appendix A: Field protocol for willow mapping plots

A.1. General

The protocol generally follows the EVMP willow monitoring protocol for macroplots with some adjustments to speed data collection and adds additional cover estimates. Macroplots are the same four-meter squares as in EVMP, with corners to the north, east, south and west of the center.

Macroplots should be fully located within homogeneous vegetation patches. Ideally there should be a five meter or greater buffer on all sides of the plot while still remaining inside the patch, requiring a homogeneous patch of at least 14 m in each dimension. See Appendix 1 for more details.

Compass azimuths should be oriented with respect to true north, i.e., they should be taken using current magnetic declination values. This applies for all purposes (laying out plots, taking cardinal direction photos, and doing plot diagrams).

A.2. Plot protocol

Plots do not need to be permanently marked, but pins and/or flags will likely be useful while sampling. The field crew can decide whether to lay out tapes or string along all sides or just measure from the center to the corners (it should be 2.83 m from plot center to each corner). Some slop on the corner locations is fine since the plots should be in homogeneous patches anyway.

Plot names should be unique and should consist of the letter M (for mapping) followed by a 3-digit number. M001 could be the first plot collected. Crews working separately can reserve blocks of numbers.

Follow the EVMP protocol to record location, observers, date, dominant willow type, ecosystem type and notes on beaver and moose presence. Add general comments if needed (obvious disturbance or any irregularities in data collection), but notes on how to revisit are not needed.

Because we'll be lining these up with high-resolution imagery and willow characteristics may vary over fine scales, spatial accuracy is key! An accurate GPS location and other spatial information for verifying location are very important.

Record the location of the plot center in UTM Zone 13 coordinates (NAD83 datum), as well as the GPS accuracy. The submeter-accuracy GNSS Arrow should be used if possible; if a less accurate unit must be used, take steps to make the reading as accurate as possible (e.g., average over a couple of minutes).

Fill out the Willow Plot Diagram sheet from EVMP. Please include anything in the immediate area that is likely to show up in aerial imagery (e.g. bare/barer patches, trees, boulders) along with an azimuth and distance from plot center. Vegetation should be included if it is likely to be visible in aerial imagery (e.g., a big conifer or dense herbaceous patch).

Follow the EVMP protocol for plot photos (two from each corner, with and without placards).

For each sampling region (e.g. a group of plots all in the same valley), draw an overview map of how the plots relate to each other and large identifiable features in the area (e.g. streams, conifer patches, big boulders). Spend no more than 10 minutes on this. NOTE: This step might be helpful to complete while you decide in advance where different plots would be valuable (see plot selection guidance in Appendix 1). However if that's not needed, and you feel the individual plot diagrams have documented the area sufficiently, this step can be considered optional. If the individual diagrams are sketchy, this could help to compensate.

Follow the EVMP macroplot protocol to record the species, width, diameter, percent in plot, height to tallest bud scar, and maximum height of each shrub. To save time, only record willows that have a maximum diameter or height > 10cm. Non-willow shrubs don't need measurements at all. For each measured willow, also estimate percent cover of live growth within the rectangle made by the max diameter and perpendicular diameter, excluding canopy gaps > 5 cm.

A.3. Cover estimates

Overview: Visual estimates of cover amounts will be used to give a reasonable idea of vegetation abundance and structure. The idea here is to visually estimate the aerial extent (the area that would be shaded by leaves and stems if the sun were straight overhead) for each functional group of plants.

Crew calibration: Before splitting up into individual field crews, have the whole crew practice together to get a sense of what various covers look like on the ground. Cover estimates should be made independently by each crew member and then discussed to form a consensus answer, both in training and at each plot.

Abiotic, dead & non-vascular vegetation: Estimate percent cover of the following abiotic and ground cover categories. For everything in this section, only record if there is at least 5% cover in the plot with a sky view—exception: water should be recorded any time it is present.

Moss or lichen	Only include if it has a sky view, including on rock that was counted already.
Coarse dead organic matter	Coarse woody organic material > 5 cm diameter, rooted dead or detached and on the ground.
Fine dead organic matter	Dead organic material < 5 cm diameter, rooted dead or detached and on the ground. Don't include litter from the current years growth.
Rock	Rocks > 2.5 cm diameter. Moss and lichen cover don't count against the rock total.
Bare soil	Mineral soil or fine gravel, < 2.5 cm diameter.
Water	Standing or flowing water above the ground surface.

Vascular vegetation: Estimate percent of the plot covered by live growth (leaves and current year's twigs) in the following functional groups. Record the most abundant three species with at least 5% cover in each group. Genus level calls are ok if you don't know the species. Please don't spend more

than 5 minutes on identification per plot, it's better to skip this step and get another plot than be sure on the non-willow identification. For cover purposes, a "tree" is defined as woody vegetation of a species that can attain 3 m or more in height and has a single main or at most only a few stems (willows that meet these criteria should also be excluded).

Willow	Live cover of all willow species.
Non-willow shrubs	Live cover of all non-willow shrubs.
Conifers	Live cover of conifers overlapping the plot, whether or not they are rooted in the plot.
Deciduous trees < 2 m tall	Live cover of non-willow deciduous trees (e.g., quaking aspen, narrowleaf cottonwood, birch and alder trees) < 2 m tall.
Deciduous trees > 2 m tall	Live cover of non-willow deciduous trees (e.g., quaking aspen, narrowleaf cottonwood, birch and alder trees) >= 2 m tall.
Total forbs and ferns	Live cover of forbs and ferns (and any other non-graminoid herbaceous vascular vegetation).
Overtopped forbs and ferns	What percent cover (of the total plot) is forbs and ferns overtopped by shrubs (willow or otherwise)? To the nearest 5% is fine.
Total graminoids	Cover of all graminoids (grasses, sedges and rushes).
Overtopped graminoids	What percent cover (of the total plot) is graminoids overtopped by shrubs (willow or otherwise)?

- You can estimate percent cover by mentally clumping the plants into one area and figuring out how big it would be. For reference, a one-meter square is equivalent to about 6% of the macroplot, and a 40-cm square is equivalent to 1%. Keep in mind that tall skinny plants viewed from the side look like they cover more area than they do from above. See references for various arrangements of cover on the following pages.
- The larger the cover value, the less an individual percentage point either way will make a difference in the end result. You are welcome to bin covers to the nearest 5% for covers over 20%.
- As with the EVMP line intercept, small gaps in the canopy of a larger plant (those less than 5 cm diameter) can be ignored, but do account for larger gaps or dead limbs.

A.4. Plot selection guidance

Plots should be collected in patches with willows, and **also in patches apparently capable of supporting willows in the future** (e.g., riparian or wet meadow settings, etc).

A good plot is centrally located within a homogenous vegetation patch of at least ten meters (preferably 14 m) in each dimension. Homogeneity should be considered with respect to cover of dominant functional groups (e.g., cover of willows and herbaceous vegetation should remain within 20% of so of the patch mean value across the patch). Plots should have no more than 15% cover of a distinct inclusion (e.g. stream channel with running water, conifer, large rock).

There should be at least a three meter buffer on each side of the macroplot while still remaining in the patch, and ideally five meters. Plots should be at least 20 m apart (more would be good, but only if homogeneous patches are large enough to permit greater separation).

Within any particular sampling region, try to collect a variety of dissimilar plots. In general it is better to spend time sampling vegetation rather than traveling; also, having dissimilar plots nearby each other provides good training data for models because all the extraneous variation that can occur between different regions is minimized when plots are nearby each other.

In any sampling region, try to locate plots to capture the range of variation present with respect to the variables listed below. (In general, if cover of willows or of other riparian shrubs, conifers, broadleaf trees, forbs or graminoids vary by 30% or more in absolute cover amounts, it is worth putting an additional plot in if homogeneous patches meeting the above requirements are present.)

High priority for additional plot (first spend time on these)

- Willow absent, but in suitable or at least borderline habitat
- Willow cover varies by 30% (e.g., one patch has 10% cover and adjacent patch has 40%, one patch has 50% cover and adjacent has 80%)
- Willow height varies by a factor of x2 (e.g., one patch has willows 1.5 m tall; adjacent has willow > 3 m tall or < 0.75 m tall)
- Willow health varies dramatically (this will probably be reflected in cover variations though). Sad willow can be heavily browsed or has died back, with more than 30% reduction from peak cover.
- Non-willow riparian shrub with > 40% cover and willows < 10% cover

Medium priority for additional plot (spend time if available)

- Conifers present vs absent, or with at least 30% more or less cover than in nearby plots
- Broadleaf trees present vs absent, or with at least 30% more or less cover than in nearby plots
- Forbs with at least 30% more or less cover than in nearby plots
- Graminoids with at least 30% more or less cover than in nearby plots
- Large differences in soil moisture from nearby plots

A.5. Cover estimate guides

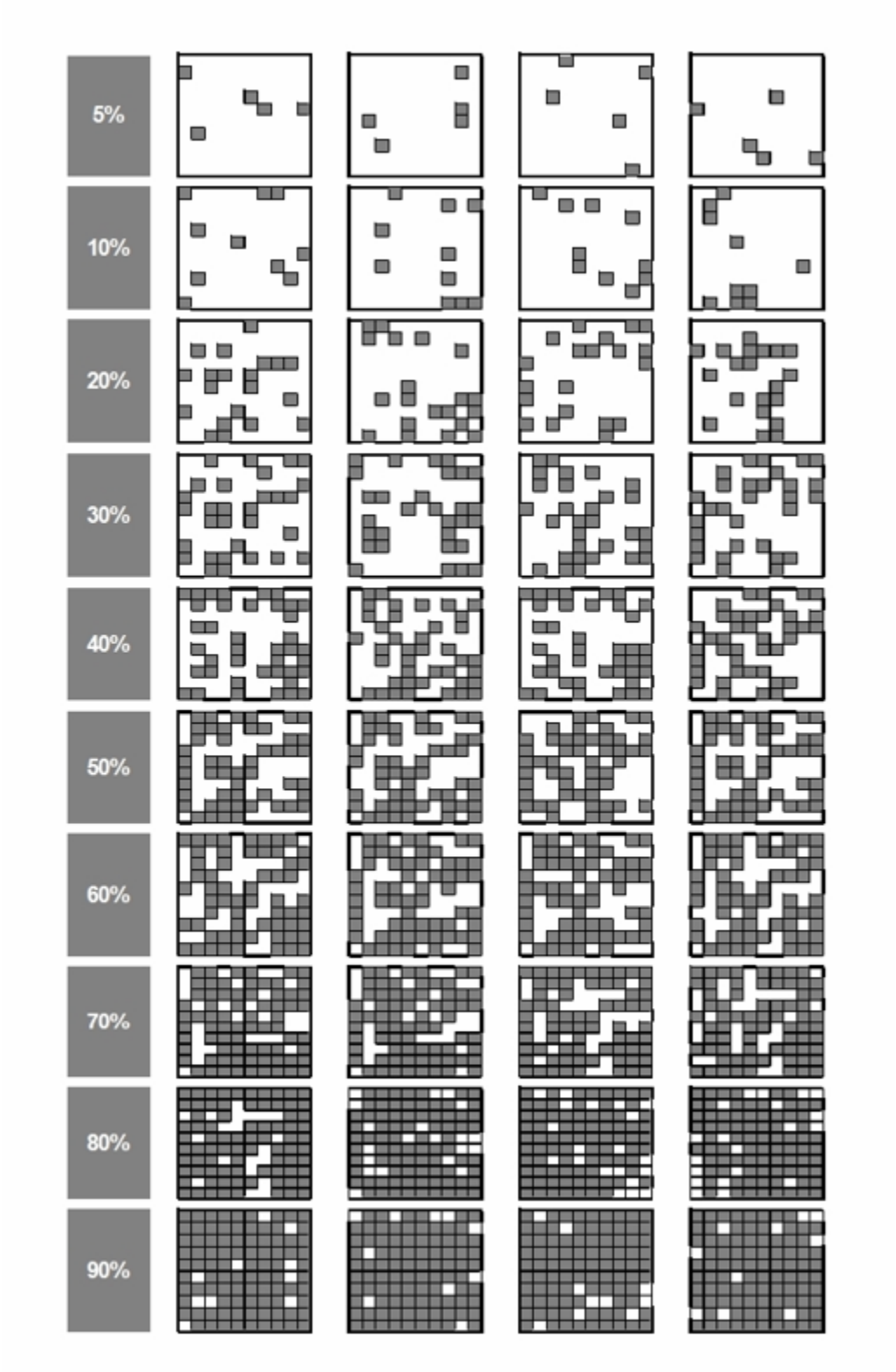

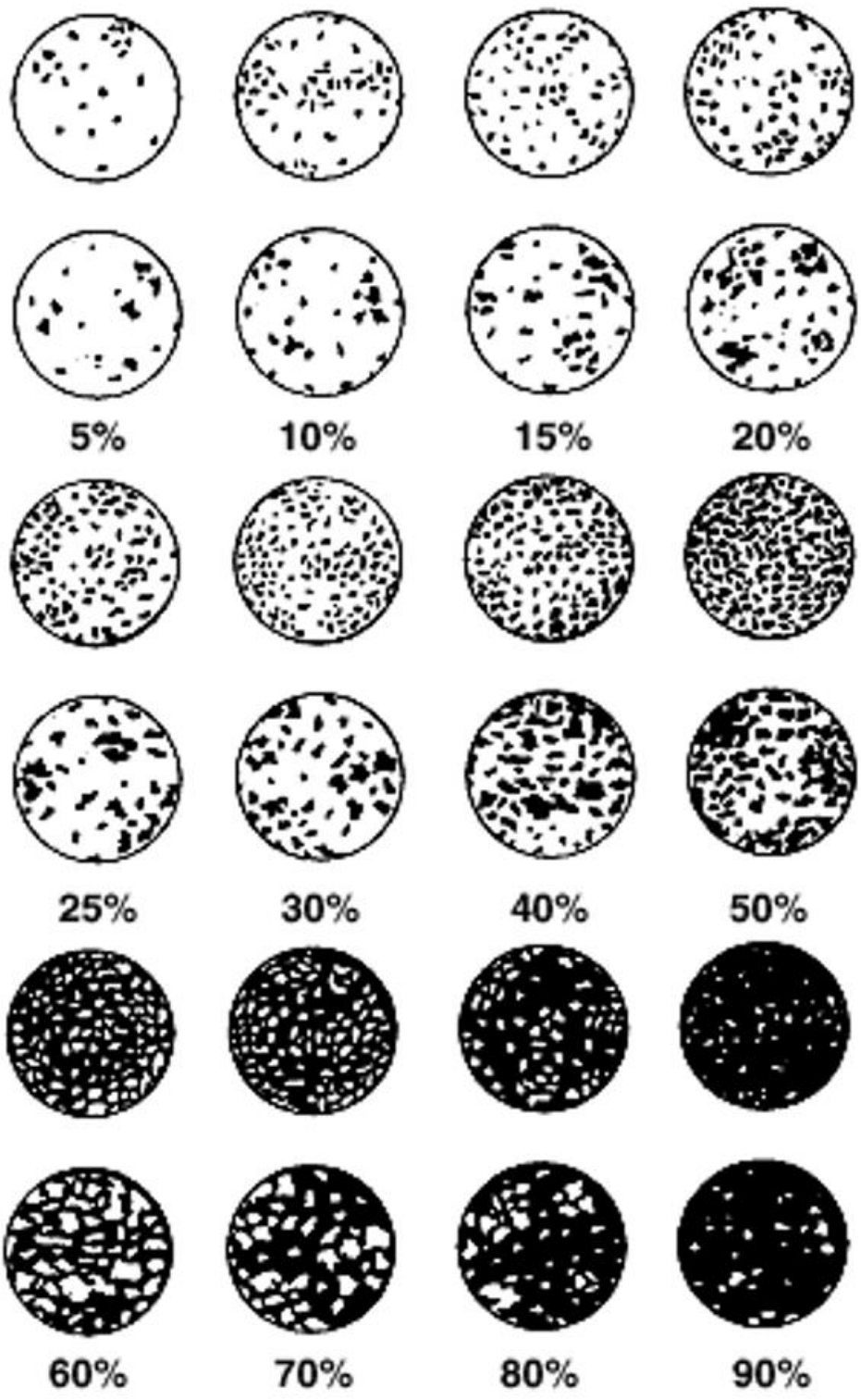
5%
10%
15%
20%
25%
30%
40%
50%
60%
70%
80%
90%

Appendix B: Leaf point intercept sampling

This protocol provided the only source of measured LAI available for use in the project. The procedure was developed for use in subalpine willow stands, but was also used in montane willow plots done in the latter part of the 2021 field season.

B.1. Overall plan

In sampling subalpine willow, we need to save time but still get some basic data that will be representative of willow productivity, in addition to the cover estimates that are spelled out in the other part of the protocol. We've come to the conclusion that we need to drop the regular EVMP protocol as it's too time-consuming in these stands. We're thinking that the quickest and most repeatable way to do this is probably going to be the following point intercept plan.

B.2. Plot layout

The plot can be laid out[44] using 4 poles, a 14-meter long string, and a 1-2 meter long string with a weight tied on the end (big metal washers could work) . The poles should be at least as tall as the tallest willows to be sampled using this protocol—extendable hiking poles[45] would be fine. The 14-meter long string[46] should be tied off in advance with a knot approximately every 1.5 m (these only need to be accurate within +/- 10 cm). The weighted string should be marked off in 10-cm intervals[47] in some recognizable way (different color adhesive tape? adhesive tape and marker? flagging tape and marker?).

Two zigzag transects are used as in the figure below, they should be done one following the other. The first (Transect A, green with blue dots below) starts at the north plot corner, and the second (Transect B, red with orange dots) starts at the west plot corner. Each transect winds thru the 4 plot corners using a different path. The transects are laid out using the 14-meter long string, tied off on the first pole just above the level of the highest canopy in the plot (or lower if need be), and remaining at about that elevation above the ground along its whole route.

[44] Feel free to sub the gear you already have for these, but see comments below about other approaches.

[45] If you've got some other poles you're already using that would work by all means use them.

[46] You could use a tape measure for this purpose and sample every 1.5 meters, but it may be more difficult to lay it out and to make unbiased vertical projections above each sample location.

[47] You could use a graduated pole for this, but see comment below.

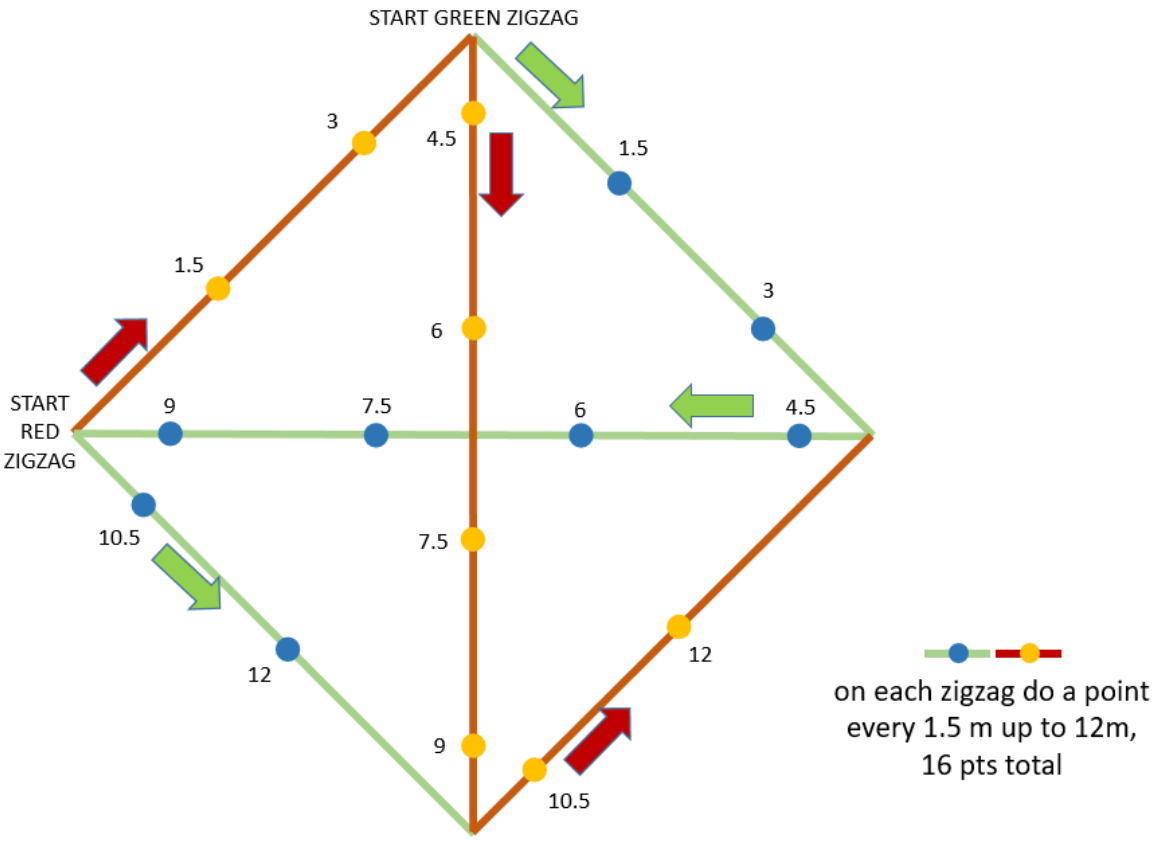
START GREEN ZIGZAG
3
4.5
1.5
1.5
3
6
START
RED
ZIGZAG
9
7.5
6
4.5
10.5
7.5
12
12
9
10.5
on each zigzag do a point
every 1.5 m up to 12m,
16 pts total

B.3. Point intercept sampling

Point samples are taken at each pretied knot by dangling the weighted string from the knot[48] so the weight is at ground level. The string should not interfere with the natural position of any stems or shoots. At each point, note the number of leaves touching the string, and the minimum and maximum height from the ground of the leaves contacted, rounding the height of each leaf to the nearest 10 cm. For example, if leaves are contacted at 23 cm, 35 cm and 48 cm from the ground, you would note 3 leaves, in the range 20-50 cm.[49]

Individual points are located at approximately the distances given in the following table from the beginning of the zigzag transect. The points in the first transect should be notated as A1–A8, second as B1–B8.

Point #	Distance (m)
1	1.5
2	3.0
3	4.5
4	6.0
5	7.5
6	9.0
7	10.5
8	12.0

B.4. Other data

Because leaves oriented away from the horizontal plane (i.e. sticking up in the air) will cause this method to underestimate leaf area, we need to have some idea whether that is an issue. So also please estimate the ***average*** angle away from the horizontal that leaves are oriented at[50] (for example, if leaves were sticking almost straight up or down this might be 80 degrees, and if they were on just a slight angle from the horizontal this might be 10 degrees).

In using this data in some kind of allometry, we might need to have an estimate for average leaf size. Similar to the leaf angle, just ballpark an overall average leaf length and width.

---

[48] We're going to use this to count the number of leaf intercepts and also know how high from the ground each is. You could use a graduated pole for this, but it will be more difficult to make unbiased vertical projections down from above (or up from the ground if using a tape measure).

[49] If it seems about as easy to do, you could just note the height of each leaf. We were concerned that sometimes there might be many leaves, making a range a lot easier to do. You also don't have to round to nearest 10 cm if that doesn't make things any easier. We'd appreciate your thoughts about both of those possibilities.

[50] This is a total guess, I'm not really sure what the best way to do this is, but it could be an important factor for estimating LAI or even in comparing plots collected at different times of day or season, if leaves start to orient to the vertical due to moisture stress. Would definitely appreciate feedback. I know it could be a challenge to estimate an average angle. Just take a guess...